

Regional transport of aerosols from Northern India and its impact on boundary layer height and air quality over Chennai, a coastal megacity in Southern India.

Saleem Ali¹, Chandan Sarangi^{1*} and Sanjay Kumar Mehta²

¹Department of Civil Engineering, Indian Institute of Technology Madras, Chennai, 600036, India

²Atmospheric Observations and Modelling Laboratory (AOML), Department of Physics and Nanotechnology, SRM Institute of Science and Technology, Kattankulathur, 603203, India

*Correspondence to: Chandan Sarangi (chandansarangi@civil.iitm.ac.in)

Abstract. Anticyclonic wind circulation is prevalent over India during winter season, causing air masses to advect from the heavily polluted North India towards south-eastern coastal regions of India and the Bay of Bengal. Here, we use a synergy of satellite, radiosonde and ground-based measurements to characterize this phenomena of these regional aerosol transport event (RTE) and their impact on the boundary layer height and air quality over Chennai, a tropical South Asian megacity. The long-term satellite data and back-trajectory analysis enables us to detect occurrence of RTEs over Chennai, which can span for 2-44 days duration. The transported aerosol layer is generally located at elevated altitudes ~1-3 km along the eastern coast of India. The duration of these RTEs in winter season over Chennai accounts for ~10-15 percent of the days and their occurrence is increasing since last 10 years. Radiosonde analysis using five sites within the transport pathway illustrates distinct aerosol-associated warming (1 to 2 K) at altitudes corresponding to these elevated layers and hence strong enhancement in lower tropospheric stability during the RTEs. In agreement, the regional aerosol/haze transport significantly reduces the boundary layer height to less than 1 km compared to background clean days (~2-2.5 km) over the east coast. Consequently, an increase in PM_{2.5} concentration over Chennai is observed (~50-55%) during RTEs compared to background days. This study provides robust observational evidence on the importance of regional transport of aerosols on air quality of downwind megacities and warrants more observational and modelling studies in future.

1. Introduction

Atmospheric aerosols are pivotal in regulating Earth's climate systems by influencing radiation budget, cloud properties and biochemical cycles. Direct and indirect effects of aerosols on the radiation balance of the Earth-Atmosphere system are evident (Comstock and Sassen, 2001; Haywood and Boucher, 2000; Lohmann and Feichter, 2005; Sathesh and Krishnamoorthy, 2005; Yu et al., 2006) and it is believed to generate climate perturbations on a regional and global scale. Apart from the local generation, the long-range transport of aerosols from their sources can severely pollute a large area far from the apportionment and it is mainly influenced by the atmospheric circulation and aerosol lifetime. Although local emissions contribute mainly to hazy episodes in megacities, it can also be influenced by regional pollutant transports (Ma et al., 2020; Mhawish et al., 2022). Such hazy events can cause severe air pollution, adversely affecting public health. Prolonged haze events and associated high PM_{2.5} loading have frequently been reported over South Asia and China during recent autumn and winter

Deleted: north India extending to south India is observed to cause

Deleted: r

Deleted: Westerly driven regional transport of aerosols from the heavily polluted North India towards south-eastern coastal regions of India across ...nd the Bay of Bengal during winter season... is a prevalent phenomenon during the winter season. ...ere, we use a synergy of satellite, radiosonde and ground-based lidar ... [1]

Deleted: Lidar

Deleted: ...easements to characterize thisese...phenomena of the ...hese regional aerosol transport events...(RTE) phenomena ...nd its ...heir impact ...n the downwind ...oundary layer dynamics ...eight and air quality over ...nd air quality over Chennai, a tropical South Asian megacity, are investigated... The long-term satellite dat ... [2]

Moved (insertion) [5]

Deleted: RTE

Deleted: regional transport events...over Chennai, wh ... [3]

Deleted: ...The duration of these RTEs in winter seas ... [4]

Deleted: 1

Deleted: 3

Deleted: per

Deleted:

Deleted: cent

Deleted: winter season

Deleted: thier

Deleted: .

Deleted:

Deleted: The occurrence of these regional transport ev ... [5]

Moved up [5]: The transported aerosol layer is generally

Deleted: 5

Deleted: time in southeastern India which are associat ... [6]

Deleted: .

Deleted: around ...1-3 km along across ... [7]

Deleted:

Deleted: entire south

Deleted: eastern

Deleted: , capped by the strong atmospheric temperatu ... [8]

Deleted: t

Deleted: T

Deleted: he

Deleted: (ABL-H) by ~38% ...o less than <... km ... [9]

Deleted: ~...3...-53...%) mainly during evening per ... [10]

Deleted: in association with the strong heating aloft ... [11]

Deleted: in future

Deleted: amics

Deleted: .

214 seasons (Qin et al., 2016; Yang et al., 2020; Zhang et al., 2021a). The significant factors influencing such hazy
215 events were attributed to stable synoptic conditions with weak surface winds and low Atmospheric Boundary
216 Layer Height (ABL-H) (Wang et al., 2014) along with the regional aerosol transport and Atmospheric Boundary
217 Layer (ABL) interaction (Zhang et al., 2015).

Deleted: (ABL) height

Formatted: Not Highlight

Deleted: ABL

218 Such transported aerosol layers, stratified above the ABL, can significantly affect the surface energy
219 balance and ABL dynamics owing to their interaction with incoming solar radiation (Ding et al., 2016; Ma et al.,
220 2020). Depending on the dominant aerosol species, the net impact of these layers could be absorbing or scattering
221 of incoming solar radiation. In either case, the presence of this transported aerosol layer can induce cooling at
222 altitudes below the layer and warming around and above the altitudes where they are located. Simultaneously,
223 near-surface accumulation of absorption aerosol concentration (under a shallower boundary layer) can lead to
224 lower atmosphere warming and surface cooling. Thus, a series of thermodynamical effects can ensue disrupting
225 stability and enhancing the upward transport of heat and aerosol through turbulent motion (Barbaro et al., 2014;
226 Huang et al., 2018). In continuation, previous studies found the role of aerosol on the suppression of ABL
227 development through their relative heating and cooling in the upper atmosphere and surface, respectively (Liu et
228 al., 2019; Petäjä et al., 2016; Wang et al., 2019b, 2020, 2018; Wilcox et al., 2016; Zhao et al., 2019; Zou et al.,
229 2017).

Deleted: ¶

230 Hence, understanding and characterising the regional transport of aerosols on the ABL structure and air
231 quality are complex. There are studies signifying the role of aerosols on the boundary layer dynamics (Aruna et
232 al., 2013; Huang et al., 2018; Ma et al., 2022; Miao and Liu, 2019; Raatikainen et al., 2014); however, most of
233 them are based on the modelling framework, and observational evidence is scarce. This study aims to delineate,
234 for the first time, the effects of transported aerosols from north India towards the southern part of the Indian
235 peninsula on the boundary layer dynamics and hence the pollution dispersion using collocated high-resolution
236 lidar, radiosondes, surface weather observations along with space-based observatories.

237 The Indo-Gangetic Plains (IGP), the densely populated and growing economy of the Indian subcontinent,
238 experiences high aerosol loading both around the surface and in the vertical column during the winter season
239 attributed to the wide range of anthropogenic activities ranging from biomass, fossil fuel burning and agricultural
240 activities (Prasad et al., 2006; Ramanathan and Ramana, 2005; Tripathi et al., 2006). The prevalence of a high-
241 pressure system over the central Indian landmass, especially during the winter seasons (December to March),
242 generates a persistent northeasterly offshore flow (Krishnamurti et al., 1998). It provides a pathway for
243 transporting aerosols from continental areas into the otherwise pristine ocean, covering thousands of kilometres
244 in less than ten days (Krishnamurti et al., 1998; Rajeev et al., 2000). As such, pollutants from North India can get
245 transported to the Bay of Bengal and then towards South India under the influence of prevalent strong convection
246 and anticyclonic cyclonic circulation formation over the northwest of the Bay of Bengal (Prijith et al., 2016;
247 Rajeevan and Srinivasan, 2000). Such transboundary transport of pollutants is evident in widespread pollution
248 over the southern Indian peninsula (Ananthavel et al., 2021b; Kant et al., 2023; Mehta et al., 2023; Mhawish et
249 al., 2022; Ratnam et al., 2018; Thomas et al., 2021). There is a campaign-based investigation held over the Indian
250 Ocean, e.g., the Indian Ocean Experiment (INDOEX) (Ramanathan et al., 1995) to investigate the characteristics
251 of transported aerosols towards the Indian Ocean and the Arabian Sea (Chester et al., 1991; Prodi et al., 1983;
252 Savoie et al., 1989). The studies revealed that the transported aerosol predominantly consists of black carbon,

organics, sulfate, nitrate, ammonia, sea salt, and mineral dust (Ramanathan et al., 2001). An increase in the aerosol loading in the free troposphere reduces the amount of incoming solar radiation reaching the surface, thus causing dimming while warming the mid and upper troposphere and cooling the surface (Dipu et al., 2013; Sarangi et al., 2018). On the other hand, they significantly alter the atmosphere's underlying thermodynamics, leading to modifying the boundary layer structure. Hence, it is essential to characterise such transports, especially their occurrence characteristics and the nature of the aerosols present. However, observational evidence on such transboundary aerosol transports, their frequency of occurrences, their impact on the ABL development and the regional pollution maintenance have not been attempted yet; this study primarily focuses on unravelling such aspects.

Here, long-term satellite observations from Moderate Resolution Spectroradiometer (MODIS), Cloud-Aerosol Lidar and Infrared Pathfinder Satellite Observatory (CALIPSO) and back-trajectory analysis are used to understand better and characterise the spatiotemporal variability in long-range regional transport of aerosols from North India to central-southern India during the winter season. Further, we have also used ground based observations of Micro Pulse Lidar, Radiosonde, surface weather and surface PM_{2.5} measurements to (i) investigate and characterize these regional aerosol transport episodes over east coast of India, (ii) quantify the associated changes in the air temperature profiles, lower tropospheric stability, ABL-H over the east coast region and (iii) quantify the associated changes in the surface PM_{2.5} distributions due to ABL-H reduction over Chennai. Section 2 describes the datasets used, followed by the methodology for composite analysis of aerosols during the Regional Transport Episodes (RTE) days and clear days. Further, results and discussion are provided in section 4 and the conclusion in section 5.

2. Dataset and Methodology

Space-based observations

MODIS on board the polar orbiting sun-synchronous satellites (Terra and Aqua) is utilised to estimate the aerosol optical depth (AOD) information at 550 nm. The MODIS measures radiance at 36 spectral bands in the visible to thermal IR spectral range of 0.41-14 μm (Kaufman et al., 1997). Within the spectral range, 7 bands are dedicated for aerosol measurement having a spatial resolution of 250m/500m. Owing to its large spatial swath (2330 km), MODIS is capable of observing the entire globe in a single day during two different times, i.e., at 01:30 AM/PM (Aqua) and 10:30 AM/PM (Terra) local time, which crosses the equator. We used the current version of Multiangle Implementation of Atmospheric Correction (MAIAC), which retrieves the AOD over land and ocean at 1 km resolution (Lyapustin et al., 2011b, 2011a), between December and March during 2015-2024 in this work.

In addition, the space-based lidar observation, Cloud-Aerosol Lidar with Orthogonal Polarization (CALIOP, (Winker et al., 2009; Young et al., 2013) onboard CALIPSO is utilised to understand the vertical variation of aerosol extinction profiles. The level 2, 5 km (horizontal averaged) standard aerosol profile (AProf) version 4.51 at 532 nm during December – March between 2015 and 2023, segregated during the RTE and clear days, are used. The CALIPSO crosses the equator ~01:30 AM/PM; we used both the day and night passes, around ± 5 degree over the eastern coastal box (as shown in Fig.1a), for the present study.

In situ observations

Deleted: and

Deleted: collocated groundbased

Deleted: over Chennai

Deleted: the widespread haziness over Chennai due to

Deleted: and

Deleted: surface meteorology

Deleted: air

Deleted: and

Deleted: ,

Deleted: ABL height (ABL-H)

Deleted:

Deleted: 2024

Deleted: however, only the night passes (~01:30 AM) are used for the present study owing to the better signal-to-noise ratio.

309 The Micro Pulse Lidar (MPL), an elastic backscatter dual-polarization lidar of Droplet Measurement
310 Techniques (DMT, USA), is located at the premise of SRM IST ([12.80N,80.0E](#), 45m above mean sea level). The
311 instrument is set up at the Atmospheric Observation and Modelling Laboratory (AOML, 40m above the ground
312 level), at a total height of 85m above mean sea level. The Normalised Relative Backscatter (NRB), [between](#)
313 [January and February during 2018 and 2023](#), is primarily utilised to retrieve total attenuated aerosol extinction
314 and determine ABL-H. Details on site description and technical specifications about the MPL (Ali et al., 2022),
315 retrieval of extinction coefficient and AOD (Ananthavel et al., 2021a, 2021b) and ABL-H estimation (Kakkanattu
316 et al., 2023; Reddy et al., 2021a) are provided in references.

317 ~~The diurnal variability of ABL-H from MPL is estimated using the Wavelet Covariance Transformation~~
318 ~~(WCT) method (Baars et al., 2008; Davis et al., 2000; Pal et al., 2010; Reddy et al., 2021a), which estimates the~~
319 ~~ABL-H from lidar profiles by step changes in signals using Haar function. We have also identified the top of the~~
320 ~~transported aerosol layer (The TAL), using the differential zero crossing method (Ali et al., 2022; Mehta et al.,~~
321 ~~2023), similar to the methodology followed by (Mehta et al., 2023) to identify the elevated aerosol layer. In~~
322 ~~general, the extinction coefficient gradually decreases above the ABL. However, presence of TAL can increase~~
323 ~~the extinction values similar to as observed within the ABL. The differential zero crossing method identifies the~~
324 ~~top of the TAL using the gradient of extinction coefficient profiles. Note that, this method of TAL detection is~~
325 ~~used only when a valid ABL is identified.~~

326 Upper air and surface weather information used in this study are obtained from India Meteorological
327 Department (IMD) from the sounding over Kolkata (22.65N, 88.45E, 6m above MSL), Bhubaneswar (20.25N,
328 85.83E, 45.0m AMSL), Vizag (17.68N, 83.33E, 69.9m AMSL), Chennai (Meenambakkam) (13.0N,80.06E, 16m
329 above MSL), about 20.13 km northeast of SRM IST, Kattankulathur and Karaikal (10.9N,79.8E, 6.9m above
330 MSL). The radiosonde data archived at 05:30 LT between December-January 2015 and 2024 are used to interpret
331 the meteorological conditions during the aerosol transport periods and ABL-H determination. [The ABL-H is](#)
332 [estimated from the potential temperature profiles, obtained from the Radiosonde. The ABL-H is the altitude at](#)
333 [which the maximum potential temperature gradient observes at the lower troposphere.](#)

334 Hourly PM_{2.5} measurements are routinely made at the U.S. Embassy and Consulate, Chennai using a beta
335 attenuation monitor (San Martini et al., 2015). The dataset within the study period ([December – January 2015 and](#)
336 [2024](#)) is obtained from AirNow (<http://www.airnow.gov>). The PM_{2.5} observations from the U.S. Embassy are
337 validated and in good agreement with other observations (Jiang et al., 2015; Mukherjee and Toohey, 2016). The
338 datasets are used to investigate the distribution of surface pollution during the haze transport from IGP to Chennai.

339 [Reanalysis datasets and back-trajectory analysis](#)

340 ~~The Modern Era Retrospective analysis for Research and Application, Version 2 (MERRA2) is employed~~
341 ~~to understand the spatial variation of Total Aerosol Extinction (TAE), radiation flux and wind parameters (U, V~~
342 ~~and resultant wind speed ($\sqrt{U^2 + V^2}$)). The MERRA2 reanalysis product provided by NASA's Global Modeling~~
343 ~~and Assimilation Office (GMAO) is available at 0.5° x 0.625° spatial resolution (Gelaro et al., 2017). MERRA2~~
344 ~~simulates five aerosol species, including sulfate, black carbon, dust, organic carbon and sea salt, with Goddard~~
345 ~~Chemistry, Aerosol, Radiation and Transport (GOCART) model and their simulated properties are found to be~~
346 ~~robust (Randles et al., 2017). We used datasets between December and March during 2015-2024.~~

Deleted: ¶

Deleted: Identification of ABL-H and top of the Transported Aerosol Layer (TAL)¶

Deleted: (

Deleted: Reddy et al., 2021; Davis et al., 2000; Pal et al., 2010; Baars et al., 2008)

Deleted: The

Deleted: is identified

Deleted: (

Formatted: Font: 10 pt

Deleted: Mehta et al., 2023; Ali et al., 2022)

Deleted: Mehta et al., 2023

Deleted: ¶

Deleted: Chennai,

Deleted: located

Deleted: at

Deleted: The gradient of potential temperature is utilised for the ABL-H determination (Mehta et al., 2017)

Deleted: , where it is the altitude of the maximum potential temperature gradient at the lower troposphere (Mehta et al., 2017)..

Formatted: Font: 10 pt

Deleted: MERRA2 Reanalysis Data Products¶

Deleted: , Speed).

Formatted: Font color: Custom Color(RGB(24,30,255))

Formatted: Font color: Custom Color(RGB(24,30,255))

Formatted: Font color: Custom Color(RGB(24,30,255))

Formatted: Font color: Custom Color(RGB(24,30,255))

Formatted: Font color: Custom Color(RGB(24,30,255))

Formatted: Font color: Custom Color(RGB(24,30,255))

Formatted: Font color: Custom Color(RGB(24,30,255))

Deleted:

370 The Aerosol Direct Radiative Forcing (ADRF) at the surface is estimated from the radiative fluxes,
 371 provided in the MERRA2 product 'M2T1NXRAD', by taking the fluxes with aerosols and without aerosol under
 372 clear sky condition. The variables SWGNTCLR (surface net downward shortwave flux assuming clear-sky),
 373 SWGNTCLRCLN (surface net downward shortwave flux assuming clear-sky and no aerosol), LWGNTCLR
 374 (surface net downward longwave flux assuming clear sky) and LWGNTCLRCLN (surface net downward
 375 longwave flux assuming clear-sky and no aerosol) are used to calculate ADRF at the surface (Thomas et al., 2019,
 376 2021).

$$ADRF = (SWGNTCLR + LWGNTCLR) - (LWGNTCLR + LWGNTCLRCLN)$$

378
 379 The Hybrid Single Particle Lagrangian Integrated Trajectory (HYSPLIT) Model is used to compute the
 380 air mass backward trajectories (Rolph et al., 2017; Stein et al., 2015). We used web-based HYSPLIT model
 381 (<https://www.ready.noaa.gov/HYSPLIT.php>) to estimate the 5- day backward trajectories reaching Chennai, to
 382 understand the pathways of aerosol transport from northern India. The Global Data Assimilation System (GDAS)
 383 meteorological data sets at a spatial grid of 1.0° were used as input to simulate the air mass backward trajectory.
 384 The trajectory height was set at every 0.5 km between surface (50m) and 4.0 km, with backward trajectories
 385 calculated at 6-hr intervals for the aerosol transport days and clear days. The trajectory density was determined
 386 by counting the number of trajectories crossing each grid cell separately.

387 Methodology

388 Composite analysis of RTE and Clear days

389
 390 The RTE days are, by definition, the days with significant aerosol transport from North India to south-
 391 coastal India, inducing a widespread haziness over the eastern coastal box. Hence, the daily AOD values over the
 392 East Coast and nearby Bay of Bengal (black box in Fig.1a), referred to as "eastern coastal box" is expected to
 393 have extreme values during RTE days. The variability in MODIS-observed daily AOD values within the east
 394 coast box was analysed and it was found that AOD values equal to 0.7 and 0.3 represent the 70th and 30th percentile
 395 values, respectively. Accordingly, RTE days are the extreme event days when domain mean AOD is greater than
 396 0.7. Conversely, the days when mean AOD values averaged within the east coast region are less than 0.3 are
 397 classified as 'clear' days. Manual inspection of all the identified days (RTE and background) was done for
 398 confirmatory check of the visible long-range aerosol transport from the IGP towards the south Indian peninsula is
 399 observed (similar to the case shown in Supplementary Fig. S1 for a reference). Many days in both composites has
 400 cloud contamination present, hence, the cloudy days over east coast box (i.e days with mean cloud fraction > 0.1)
 401 are excluded from the composites of both RTE and Background clean days. Based on both these criteria, we have
 402 119 number of RTE days and 71 number of background clean days for analysis. We used these segregated days to
 403 perform composite analysis to understand the RTE associated perturbations in aerosol vertical distribution
 404 (CALIPSO and MPLMPL observations), temperature profiles and ABL-H (IMD Radiosondes) and MERRA-2
 405 simulated Total Aerosol Extinction (TAE), surface net radiation fluxes and aerosol radiative forcing over the east
 406 coast of India (compared to background clean days). CALIPSO swaths available around the eastern coastal box
 407 (as shown in Fig.1a) are grouped with respect to the RTE and clear days to study the three-dimensional variation
 408 of extinction profiles pertinent to the RTE phenomena. Moreover, MPL (vertical profiles of extinction coefficient)

- Deleted: ¶
- Deleted: Hysplit Backtrajectory : ??¶
- Deleted: HYSPLIT Model
- Deleted: ¶
- Deleted: ¶
- Formatted ... [12]
- Formatted ... [13]
- Deleted: ¶
- Deleted: Characterisation
- Deleted: n
- Deleted: r Sky
- Deleted: By definition, the
- Formatted ... [14]
- Deleted: th and
- Deleted: The RTE days are the days with significant ... [15]
- Deleted: exceeds 0.7
- Deleted: over the East Coast and nearby regions, as ... [16]
- Deleted: .
- Deleted: Note that only days showing a visible trans ... [17]
- Deleted:
- Deleted: there are
- Deleted: without any such transports; occurrences of ... [18]
- Deleted:) and
- Deleted: termed
- Deleted: them
- Deleted: background clean
- Deleted: r
- Deleted: '
- Deleted: Note that days obscured with clouds (i.e day ... [19]
- Deleted: of
- Deleted: NET
- Deleted: ¶ ... [20]
- Deleted: during the RTE and clear days are segregate ... [21]
- Deleted: ±5° longitudes of
- Deleted: .r.t
- Deleted: background
- Deleted: an
- Deleted: spatial
- Deleted: dimentional
- Moved down [2]: in addition to the MERRA2 (spatially
- Deleted:
- Deleted: corresponding
- Deleted: events
- Deleted:

and PM_{2.5} measurements available during RTE and clear days over Chennai are also segregated into these composite days to infer the ABL-H variability and pollution concentration. Details of the sample available for the analysis are presented in Supplementary Table 1.

3. Results and Discussion

3.1 Occurrence of RTE and clear days

The mean spatial distribution of columnar AOD over the Indian subcontinent for RTE and clear days composites are compared in Fig. 1a and 1b. The significance of regional aerosol transport from north India to south is evident, as a majority of grids in the east-coastal region and a considerable portion of the Bay of Bengal has very heavy aerosol loading ($AOD > 1$). In contrast, the composite mean of AOD during clear days (Fig. 1b) is substantially lower (0.23 ± 0.06) over the eastern coastal box, as portrayed in Fig. 1b. The spatial distribution of aerosols during the RTE and clear days is further confirmed using the MERRA2 reanalysis products. The average of the MERRA2 simulated columnar AOD at 550 nm, superimposed with the wind vectors at 850 hPa, for the same composite of RTE and clear days are compared (Figure 1c-d). The analysis shows a similar pattern as observed from AOD distribution from MODIS data; however, variation in the magnitudes is present. Notably, the MERRA2 simulated columnar AOD values span from 0.6-0.9 on RTE days across the East Coast and is largely 50-60% greater compared to clear days.

The composites also show that the aerosol transport from the Indo-Gangetic Plain to the southern Peninsula via Bay of Bengal is predominantly by the divergence associated with the anticyclonic circulations prevalent during the winter season. The MERRA2 simulated wind circulation flow manifests into a northerly wind as it enters the Bay of Bengal and eventually merges into the easterly circulation (prevalent around the tropics) as the wind enters back into the southern Peninsula, south of 20°N. During the winter and pre-monsoon season, the westerlies wind system is prominent over Northern India and IGP in the lower troposphere prevalent to the high-pressure system generation over central India (Krishnamurti et al., 1998). It is worth noting that the easterly wind speed across the southern BoB is stronger during clear days than on RTE days. As such, the difference between the RTE and clear-day wind speed composites is that the wind speed during RTE days across the entire eastern half of the Indian subcontinent is weaker than the clear days (Supplementary figure Fig S3). The reduced wind speed is expected to promote the endurance of aerosols over the eastern coast column and induce greater AOD over the south-eastern coast and the southern Indian peninsula.

We further checked the wind back trajectory model to better understand the pathway characteristics. Fig. 1e and f shows the number density of HYSPLIT trajectory analysis for the RTE and clear day, respectively, between surface (50m) and 4 km, illustrating the 5-day backward trajectories reaching Chennai, computed for every 6-hour interval. It also indicates that pollutants are predominantly transported from the northern parts of India and from the IGP outflow region over Northern BoB during RTE. In addition, there also observed transport from inland areas of the eastern coasts along the anti-cyclonic circulation pathway of the aerosol flow from North India. On the other hand, the transport is predominantly from the nearby oceanic region during the clear days. Thus, this 5-day back-trajectories also confirm the fidelity of the RTE composites and that they are indeed characteristically different from the composite of background days.

Deleted: in addition to the MERRA2 (spatially across the Indian subcontinent) Total Aerosol Extinction (TAE), surface net radiation fluxes, and wind products.¶

Formatted ... [22]

Deleted: ¶

Deleted: -sky

Deleted: 10-year

Deleted: climatological mean

Deleted: , between 2015 and 2024, ...ver the Indian subcontinent from ... [23]

Deleted: cleanr

Deleted: during December

Deleted: these months is

Deleted: the ...east-coastal region and a considerable portion of the Bay of Bengal has very heavy aerosol loading ($AOD > 1$). In contrast, the composite mean of AOD during clean ...lear days (Fig. 1b) is substantially lower (0.23 ± 0.06) over the eastern coastal box, as portrayed in Fig. 1b; composite mean AOD over the entire central and southeastern India during RTE days is 0.42 ± 0.08 (Fig. 1a). The composite mean of AOD during clear days (Fig. 1b) is substantially lower (0.23 ± 0.06) over the region eastern coastal box, as portrayed in Fig. 1b; however, as expected, it was greater than 0.7 over the North India region. The RTE and clear days are observed to be 119 and 70 days, respect ... [24]

Deleted: MERRA 2...reanalysis products. The avera ... [25]

Deleted:)

Deleted: ...superimposed with the wind vectors at 8 ... [26]

Deleted: b

Deleted: -d

Deleted: c.... The analysis shows a similar pattern as ... [27]

Deleted:

Deleted: TAE exceeds 60%....6-0.9 on RTE days acr ... [28]

Formatted: Font color: Auto

Deleted: Merra...ERRA2 simulated wind circulation ... [29]

Deleted: accumulation

Deleted: Hence, w

Formatted: Font: 10 pt

Formatted: Font color: Auto

Deleted: National Oceanic and Atmospheric Adminis ... [30]

Deleted:)

Formatted: Font:

Formatted ... [31]

Deleted: originating from...eaching ... [32]

Deleted: across the BoB

Formatted ... [33]

Deleted: that ...he fidelity of the our ...TE composit ... [34]

Formatted: Font:

We also checked for diurnal pattern in the MERRA2 simulated TAE values. However, such variations are negligible, pointing to the longer duration of such events. Hence, we further examined the endurance of RTE days. Normally, the RTE events prolong for days; persistence of such events for more than a day is observed to be ~53% of total observation, while 21% of occurrences have RTE durations of more than 4 days. Duration of RTE episodes, in general, can vary from one day to 4-6 days. Overall, we have categorized RTEs as episodes of varying duration, i.e. 1 day, 2 day and so on till 5 days, and the occurrence of RTEs episodes within each category at yearly basis is recorded. Supplementary figure Fig.S2S2, provides an overview of occurrence of RTE events under each category between 2015 and 2024. On average, the RTE which occurred over the south-eastern coast box for consecutive 2-4 days is the highest (as shown in Fig.S2), and such events show an increasing pattern. Notably, the year 2022 experienced a 12-day consecutive haziness between the 20th and 31st of March. Figure S2 also suggests an increasing trend in the overall occurrence of RTE days. Endurance of such hazy periods can result in significant consequences on the air quality and boundary layer dynamics.

3.2 Vertical aerosol structure during RTE and clear days.

The CALIOP observed mean vertical distribution of the aerosol extinction over the south-eastern coastal region during the RTE days and clear days is shown in Fig.2a and b, respectively. As expected, there is a distinct decreasing gradient in aerosol extinction values between surface and 2 km altitude as we move from IGP in the north to southern peninsular coastal India during both RTE and clear days. More interestingly, high values of aerosol extinction (> 0.2) are discernible up to 5 km during RTE days over the region south of 20°N during RTE days, while the same is confined to altitudes less than 1.5 km during clear days. Also, over region north of 20°N, a relative increase in the extinction within ~1-4 km can be observed on RTE days relative to clear days. Note that, the averaged profiles cover both the land and ocean parts and there can be differences in the extinction coefficient due to the contrast between the land and ocean swaths of the CALIPSO. To understand the variations in the vertical distribution of aerosols between the RTE days and background days composites, we analysed the CALIPSO profiles over the land and sea pixels of the east coast box, separately (Figure S7, S8 and S9). The mean extinction during the RTE days is observed to be greater than 0.2 over the land, however it observes between 0.1-0.2 over the ocean region. While the land regions have high aerosol concentration near the surface, the same is not seen over ocean as there is no active surface emission sources over Ocean. However, the transported elevated aerosol layers are present at altitudes 1 to 3 km over both the land and the ocean regions.

Further, ground based MPL-observations over Chennai is used to study the RTE-associated diurnal and daily-scale perturbations in vertical distribution of aerosols over this region. We show the temporal changes in the vertical characteristics of aerosol extinction and TAL during a one week RTE episode between 23rd-29 January 2018 over Chennai (as shown in supplementary Figure Fig.S1 and S1A), as observed by MPL, is provided in Fig.2c. The temporal variation of background surface meteorology, including surface T, wind speed (WS), PM2.5 and the AOD, are provided in the Supplementary Figure Fig.S4. A significant increase in the columnar AOD between ~0.4 and 0.8 is observed during the hazy events. However, it maintains ~0.2-0.3 during the clear days. It is also worth noting that the AOD above the ABL (integrated extinction within the free troposphere) is observed to be close to the AOD values during the RTE period, suggesting a dominant presence of TAL above the ABL. The occurrence of the TAL can be seen above the ABL during the RTE periods and persisted for ~3-4 days. The top of the TAL was observed initially at ~2.5 km at ~06:00 LT (or IST) on 24 January 2018, which gradually

Formatted: Tab stops: 1.25 cm, Left + Not at 1.93 cm

Deleted: During the winter and pre-monsoon season, the westerlies wind system is prominent over Northern India and IGP in the lower troposphere prevalent to the high-pressure system generation over central India (Krishnamurti et al., 1998). This flow manifests into a northerly wind as it enters the Bay of Bengal and eventually merges into the easterly circulation (prevalent around the tropics) as the wind ... [35]

Deleted: ¶ ... [36]

Formatted: Font: 10 pt

Formatted: Font: 10 pt, Not Bold

Formatted: Font: 10 pt

Formatted: Font: 10 pt, Not Bold

Formatted: Font: 10 pt

Formatted: Font: 10 pt, Not Bold

Formatted: Font: 10 pt

Deleted: Fig. 1e

Deleted: Supplementary figure Fig.S2 provides an ov ... [37]

Deleted: Here, the number of consecutive RTE days ... [38]

Deleted: 3

Deleted: category'

Deleted: S2

Deleted: Figure S2 also suggests an increasing trend ... [39]

Deleted: Endurance is calculated as the total duratio ... [40]

Deleted: dominates the days exceedingly more than ... [41]

Deleted: .

Deleted: On average, the RTE which occurred over t ... [42]

Deleted: 3

Deleted: .3 Vertical aerosol structure during RTE ... [43]

Deleted: It is worth noting that the easterly wind spe ... [44]

Deleted: (bounded box in the dotted line in Fig.1a and b)

Deleted: -sky

Deleted: 15

Deleted: -sky

Deleted: 1

Deleted: 2

Deleted:

Deleted: Also, t

Moved up [6]: Also, the mean extinction during the RTE

Deleted: . Thus, the RTE-associated differences in ae ... [45]

Deleted: Note that, the aerosol extinction coefficient ... [46]

Deleted: Nonetheless, the above analysis of

Deleted: RTE-associated changes in

Deleted: lacks diurnal or daily resolution and also a ... [47]

Deleted: w

865 reduced to ~1.5 km and merged with the ABL at 09:00 LT on 28 January 2018. Thus, the vertical distribution of
 866 total attenuated aerosol extinction between 24th-27th January 2018 is representative of RTE and the background
 867 days (23 and 28-29 January) as clear day conditions.

868 The study further extends to the variations in the aerosol extinction during RTE and clear days. Figure
 869 2d shows the day averaged profiles of RTE (24-27 Jan 2018) and clear days (23, 28, 29 Jan 2018) observed during
 870 the typical case from MPL observations, as shown in Fig.2c. Although the extinction values are observed to similar
 871 near the surface, it rapidly decreases till ~0.8 km during the RTE days. Further, it maximizes within the altitude
 872 range ~1-2.5 km. Overall, the aerosol extinction during the RTE days is observed to be 50-60% higher than clear
 873 days between 1-2.5 km, suggesting the presence of TAL. Fig.2c also superimposed with the ABLH determined
 874 from MPL observations and temperature profiles obtained from radiosonde observation from Chennai
 875 (Meenambakkam). The observed temperature profiles indicates the top of the TAL. Interestingly, the ABL-H also
 876 decreased from ~1.4 km to ~0.3 km (~78% reduction) between 24 and 25 January 2018. The mean ABL-H is
 877 observed to be 1.3±0.8 km and 1.8±0.8 km during the RTE and clear days, respectively, exhibiting an overall
 878 reduction of ~40%. Temperature inversions are also observed near the top of the TAL during the RTE, which can
 879 also be attributed to the aerosol-induced warming of the atmosphere and large-scale circulation (Ganguly and
 880 Jayaraman, 2006; Sinha et al., 2013). However, such aspects are not addressed here due to the limited datasets.

881 3.3 RTE-associated atmospheric warming, lower tropospheric stability and ABL-H suppression,

882 To understand the effect of the transported aerosols and their vertical extent on the background thermal
 883 conditions, we also analysed the vertical temperature (T) profiles obtained from radiosonde observations:
 884 Kolkata, Bhubaneswar, Vizag, Chennai and Karaikal, located in the east coast of the Indian peninsula, as
 885 depicted in Fig.3a. The average T profiles with standard error obtained for the RTE (red) and clear (blue)
 886 categories are shown separately for different stations in Fig.3b-f. The relative difference (in percent) between the
 887 temperature profiles of RTE and clear days, from the RTE ($\frac{T_{RTE}-T_{Clear}}{T_{RTE}} \times 100\%$) is shown on the top axis as
 888 dashed lines.

889 Over Kolkata, where it lies in the northmost region, the relative enhancement in the temperature RTE
 890 ($\frac{T_{RTE}-T_{Clear}}{T_{RTE}} \times 100\%$) forms a parabolic shaped structure which was located between 0.3 km to 2 km and has its
 891 centre around 1 km and sharply decreases afterwards. Over Vizag and Bhubaneswar, the intermittent stations,
 892 similar parabolic shape in relative differences is observed, spread between 0.2-2.5 km with centre between 1 km
 893 to 1.5 km. Interestingly, Chennai and Karaikal, the south most stations, also observed observes the parabolic
 894 shape heating starting 0.5 km but the upper stretch was extended up to 3 km, with centre located between 1.5 km
 895 to 2 km. This phenomenon also suggests that aerosol-induced warming at the lower troposphere not only enhance
 896 the temperature at the altitude where aerosol occur but also modifies the overall temperature profiles of the lower
 897 atmosphere. Moreover, the observed phenomena of enhancement in altitude of RTE-associated warming as we
 898 move southward from IGP, is also consistent with the fact that the long-range transported aerosol plumes gets
 899 elevated at downwind locations (Stohl, 2006; Yu et al., 2012) (Stohl, 2006; Yu et al., 2012). Over Chennai, the
 900 altitude of observed peak warming coincides with the peak occurrence of TAL, as observed in Fig.2c, suggesting
 901 the aerosol-induced radiative effects of TAL on temperature profiles. Also, the observed warming occurs
 902 throughout the column till ~3km over both Chennai and Karaikal. This phenomenon also suggests that aerosol-

Moved (insertion) [7]

Deleted: ¶

Moved up [7]: Thus, the vertical distribution of total

Deleted: Such aerosol accumulations are followed by ... [48]

Deleted: Nonetheless, the above analysis of RTE-ass ... [49]

Deleted: ¶

Deleted: diurnal changes

Formatted ... [50]

Deleted: ,

Formatted ... [51]

Deleted: are

Deleted: during the RTE days

Formatted ... [52]

Deleted: , maximising ...etween 1-2.52.5...km, sugg ... [53]

Deleted: Such enhancement can be attributed to ...h ... [55]

Formatted ... [54]

Deleted: attributed...e attributed to the aerosol-induc ... [56]

Deleted: The temporal changes the difference of exti ... [57]

Deleted: . Fig.2d shows

Deleted: ¶

Deleted: Hence, the accumulation of the diurnal varia ... [59]

Formatted ... [58]

Deleted: On the other hand, absorbing aerosols can h ... [60]

Deleted: metrological ...hermal conditions, we also ... [61]

Deleted: and Bhubaneswar... where it lies in the nor ... [64]

Formatted ... [62]

Formatted ... [65]

Formatted ... [63]

Formatted ... [66]

Deleted: maximizes

Deleted: center

Deleted: .5

Formatted ... [67]

Deleted: such decline occurs above

Deleted:

Deleted: center

Formatted ... [68]

Formatted ... [69]

Deleted: s

Formatted ... [70]

Formatted ... [71]

Deleted: throughout the column

Deleted: center

Formatted ... [72]

Moved down [9]: Over Chennai, the altitude of observed

Deleted: .

Deleted:

Formatted ... [73]

Formatted ... [74]

Moved down [8]: The effect of the accumulated aerosol on

Moved (insertion) [9]

Deleted: On the other hand, the radiative impact of th ... [75]

Deleted: Notably

Deleted: extends

Formatted ... [76]

Formatted ... [77]

induced warming at the lower troposphere not only enhance the temperature at the altitude where aerosol occur but also modifies the air temperature near surface. Similar to the observation over Chennai, the observed heating during the RTE days over the other stations can also attributed to the presence of TAL. However, the observed latitudinal differences in the magnitudes of warming can be due to the spatial inhomogeneity of the aerosol concentrations, mainly attributed to the transport strength. Interestingly, the intensity of RTE-associated warming over megacities like Kolkata, Bhubaneshwar and Chennai are greater than that of Vizag and Karaikal, suggesting role of local emissions.

Figure 4a examines the relative differences in lower tropospheric stability (LTS i.e. gradient in the temperature between 1.5 km and surface (ΔT)) during the RTE and clear cases across the different stations over the eastern coast. During the background clear days, the LTS is largely ~ 7 K but the same during RTE days is skewed ~ 4 K suggesting the enhanced LTS, and hence atmospheric stratification. The variations in the LTS can have stronger impact on the ABL-H, and the relative suppression of ABL under the influence of the TAL are addressed in Fig.4b-c.

For ease of comparison and increase the sample size, we grouped radiosonde-estimated ABL-H data over Kolkata, Bhubaneshwar and Vizag (representing the north region of the east coast box) into one comparison plot (Figure 4b), and the observed ABLH over Chennai and Karaikal into the other plot (representative of transported plume to South region of east coast box). It is also interesting to observe a latitudinal heterogeneity in the peak occurrence of ABL-H over the east coast. The mode of distribution of ABL-H during clear day composite varies between 1.5 – 2 km over north region and the same is 2 – 2.5 km over the south region. During RTE days the distribution of ABL-H shifts drastically to lower values and the mode of distribution is decreases significantly to ~ 0.3 – 0.4 km over north region and 0.5 – 1 km over south sites suggesting the strong influence of TAL-associated LTS on suppression of ABL across the eastern coast. As an effect of the accumulated aerosol concentration above the ABL heats the thermal inversion layer and strongly suppresses the ABL development (dome effect) (Ma et al., 2020). The shallow ABL further promote severe hazy episodes (Quan et al., 2014; Ye et al., 2016).

Figure 4d. shows the mean ABL-H observed over SRM IST (Chennai) during the RTE (red, 10 days) clear days (blue, 6 days). Overall, the mean ABL-H observed during clear days and RTE days are observed to be $\sim 0.9 \pm 0.3$ km and $\sim 0.6 \pm 0.2$ km, respectively, accounting a relative suppression of ABL-H by ~ 33 – 35% during RTE days. Notably, such decrement in the ABL-H was dominant during the afternoon hours (15–19 LT), where it shows a declined from clear days (1.0 ± 0.1 km) to RTE days (0.6 ± 0.1 km) by ~ 67 – 70% . Such dominant suppression was also observable during forenoon hours (08–12 LT), accounting a reduction of $\sim 45\%$. Moreover, the ABL-H evolution is also considerably different between the two composites. While the evolution of ABL-H with time of the day is gradual during the clear days, the transition of ABL-H between midday and afternoon is much steeper during RTE days. Also, the time to reach maximum ABL-H is delayed by ~ 1 – 2 hours during RTE compared to background clear days. The suppression of the ABL followed by accumulation of absorptive aerosol in the upper ABL has been investigated earlier, especially through numerical simulations (Ding et al., 2013, 2016; Zhao et al., 2019); however, observational evidence is scarce. (Barbaro et al., 2014) suggests that a drop in the ABL from 1.4 km to 0.9 km ($\sim 35\%$ reduction), through sensitivity experiments. Similarly, (Wang et al., 2015) suggest that the stable stratification of the atmosphere above the ABL through the significant warming by absorbing aerosols contributed to a decrease of ABL-H by 33% . Observational studies over China suggest that the occurrence

Deleted: overall

Deleted: profiles of the...ear surface lower atmosphere...
Observational study by (Huang et al., 2018) over Northern Northern China region shows a significant heating in the upper ABL, where the aerosol accumulation is more, with a maximum temperature change of $\sim 0.7^\circ\text{C}$ on average. Recent studies suggest that the occurrence of the aerosol layer in lower troposphere warming while inducing a strong inhibition layer, and it may further promote extreme precipitation events (Dagan and Eytan, 2024). ¶

Formatted: Font:

Formatted

Deleted: ga

Deleted: This variation can also be induced by the ...ocal emissions.; however, such aspects are difficult to address at the moment due to the limited instrumentation.

Formatted: Font:

Deleted: Although the wind direction is north easterlies up to 3 km in both stations, the WS varies during the RTE and clear days. The WS up to 3 km is almost similar to that of Chennai and Karaikal during the RTE days except at the surface. However, it exceeded by ~ 2 m/s during clear days over both stations. The WS is observed to get stronger above ~ 1.5 km during the RTE days. Such an enhancement in the WS can favour the transport from IGP and accumulate over the boundary layer. However, the overall WS during RTE days remains calmer than on clear days. The effect of the accumulated aerosol on the boundary layer processes majorly depends on the aerosol characteristics. For instance, th

Deleted: As mentioned earlier, the occurrence of RTE

Deleted: difference

Deleted: between

Deleted:)

Deleted: Although the

Deleted: cases distribution...s largely peak maximiz

Deleted: ,

Deleted: cases

Formatted: Font:

Formatted

Formatted: Font:

Deleted: towards ~ 1 K suggesting the enhanced Low

Deleted: n, favouring the “dome effect”. ...he variati

Formatted: Font:

Formatted: Font:

Deleted: To enhance the sample size...or ease of

Moved up [10]: While the north regions show a strong peak

Moved (insertion) [1]

Deleted: It is also interesting to observe a latitudinal

Deleted: ¶

Formatted

of elevated aerosol layers has induced suppression of ABL-H from 1.27 km to 0.78 km (~38% reduction) hence lifting the surface pollution level to 118% (Wang et al., 2018). (Zhang et al., 2021b) reports a reduction in the ABL-H from 1.09 km to 0.48 (~60% reduction) during intense haze episodes over China.

Supplementary figure Fig. S6 shows the aerosol direct radiative forcing (ADRF) observed during the RTE and clear days, estimated from MERRA2 radiative flux observations at the surface (Thomas et al., 2019, 2021). Overall, the ADRF has a net cooling at the surface both during the RTE and clear days. However, RTE triggers to enhance the cooling of the surface to ~20-40 W/m². Such strong cooling observes to be around the eastern coastal regions where the aerosol transports generally occur. In specific, it reduced to less than -40 W/m² over the eastern coastal box where the TAL present. During clear days (Fig.S6b), the strong cooling is confined over the IGP alone (~-25-30 W/m²). The difference in the ADRF during the RTE and clear day composite is shown in Fig.S6c, evidencing a cooling of ~-15-20 W/m² by the RTE days. It also suggests that aerosol transport from the north India has a profound effect on the radiation and eventually on the ABL-H. The solar dimming due to the presence of TAL can block the solar radiation reaching the surface, resulting in the overall dimming in the ground surface, weakening the surface flux, perturbing the convective process and suppressing the ABL development. The development of ABL during daytime is mainly dominated by convective processes (Garraff, 1994; Stull, 1988); however, the formation of TAL suppresses such development, via reduction in the incoming solar radiation, especially the surface dimming and inducement of the “dome effect” (Guo et al., 2017; Petäjä et al., 2016). Enhancement in the suppression of ABL-H distribution during the afternoon hours can also be attributed to the thermal internal boundary layer formation, where the transport of pollutants towards the land from BoB under the influence of sea breeze (Reddy et al., 2021b). However, this contention requires further investigation with large samples.

3.4 Impact of transported aerosols on the air quality of downwind megacities

The association of ABL-H and PM_{2.5} is delineated using collocated observations of MPL and PM_{2.5} measurements over Chennai using the measurement across SRMIST and US Consulate, Chennai, respectively. Fig. 5a5a shows the scatter of normalised anomalies between PM_{2.5} and ABL-H during RTE days, showing for each 2 percentile observations. Note that, the first and last 4 percentile of the observations are excluded from the analysis to remove outliers. The normalised anomalies are obtained by subtracting the parameters from the climatological average (during the winter season) and further divided with the same ($X Anom. = \frac{X - X_{Mean}}{X_{Mean}} \times 100\%$, where X = PM_{2.5}, ABL-H). Note that, average ABL-H during the winter season is estimated with the NRB during 2018 and 2023 alone. However, it matches with the climatological ABL-H estimated by (Reddy et al., 2021a) over Chennai. As expected, the normalised anomalies between PM_{2.5} and ABL-H are negatively related, with a statistically significant (>95% confidence) correlation of -0.6. It portrays that, overall, a 30% reduction in the ABL-H can contribute to ~130-150% increase in the surface PM_{2.5} concentrations. Observational studies by (Su et al., 2020) show a nearly similar relationship during COVID-19 in China; however, with a different correlation value over Beijing and Northern China, attributed to the inhomogeneity in the spatial distribution of pollution.

Finally, the overall diurnal changes in PM_{2.5} during the RTE and clear day composites are portrayed in Fig. 5b5b. As expected, the RTE days experience ~50-55% enhancement in PM_{2.5} than clear days. During the clear

Formatted: Check spelling and grammar

Formatted: Check spelling and grammar

Formatted: Indent: First line: 0 cm

Moved (insertion) [11]

Deleted: ¶

Deleted: hence reducing the ABL-H. On the other hand,

Deleted: the complex radiative interaction between

Deleted: with the TAL,

Deleted:

Deleted: ,

Deleted: can also affect the development of ABL

Moved up [11]: The solar dimming due to the presence of TAL can block the solar radiation reaching the surface, resulting in the overall dimming in the ground surface, weakening the surface flux, perturbing the convective process and suppressing the ABL development.

Moved (insertion) [8]

Deleted: As mentioned earlier, the suppression of AH ... [91]

Deleted: ¶

Deleted: As discussed earlier, the pollutants to the se ... [92]

Moved up [1]: . Such suppression in the ABL-H was

Deleted: Interestingly, the PDF during RTE days pea ... [93]

Deleted: .

Deleted: The RTE days where MPL is operational ar ... [94]

Deleted: 4d

Deleted: .

Deleted: .

Deleted: $\frac{X - X_{ClimatologyMean}}{X_{ClimatologyMean}}$

Deleted: Interestingly

Deleted: 38

Deleted: 5

Deleted: d

Deleted: 100-

Deleted: . It is to be noted that, the wind speed and ... [95]

Deleted: In general, an increased ABL height, as usu ... [96]

Deleted: ¶

Formatted: Indent: First line: 0 cm

Deleted: b

Deleted: 4

Deleted: d

Deleted: 3

Deleted: 30-3

Formatted: Not Highlight

Formatted: Not Highlight

1872 days, the $PM_{2.5}$ increases steeply during the early morning hours and maximizes at $50 \mu\text{g}/\text{m}^3$ at 08:00 LT. This is
 1873 followed by a gradual decrease to the daily minimum value of $\sim 20 - 25 \mu\text{g}/\text{m}^3$ from 08:00 till 15:00 LT, before
 1874 increasing slightly in evening and night till $30 \mu\text{g}/\text{m}^3$. In comparison, the RTE composite mean shows similar
 1875 diurnal variability in the $PM_{2.5}$ values but the magnitudes are greater. The maximum value at 08:00 LT is ~ 80
 1876 $\mu\text{g}/\text{m}^3$ and the daily minimum value is $\sim 35 \mu\text{g}/\text{m}^3$ at 15:00 LT, followed by slight increase in evening $\sim 40 \mu\text{g}/\text{m}^3$.
 1877 As such, the percentage increase in $PM_{2.5}$ during RTE composite is more than 50% with the maximum being
 1878 around morning 0900-1100 LT of ~ 65 -80%. This is probably due to shallower ABLH over the megacity of
 1879 Chennai during winter. Note that Fig. 4c illustrated the decrease in ABLH is maximum during morning and evening
 1880 time and least during midday. The clear days, characterized by elevated ABL-H, often promote enhanced wind
 1881 speed and vertical mass movement (Xiang et al., 2019) can result reduction in the surface pollutions. On the other
 1882 hand, a suppressed ABL-H as observed during the RTE days significantly affect the vertical dispersion, leading
 1883 to higher concentrations of pollutants near the surface (Wang et al., 2019a). It is also to be noted that, the surface
 1884 pollution aggravation becomes complicated in the presence of stable boundary layer, such that, it hinders the
 1885 exchange of pollutants and energy between the surface and free troposphere and potentially leading to higher
 1886 concentration of pollutants in the atmosphere if they are not cleared otherwise (Shi et al., 2020).

1887 4 Summary and Conclusion

1888 This paper presents the first observational evidence of the effect of long-range transported aerosols on the
 1889 boundary layer dynamics and $PM_{2.5}$ enhancement over the east coast regions of peninsular India. The aerosol
 1890 transport from IGP towards south India (referred to as RTE) occurs mainly under the anticyclonic circulation
 1891 prevalent over the east coast of India and nearby BoB regions. The RTE events typically spans for 2-4 days and
 1892 are characterized by widespread haziness across the eastern coast. While the pollutant concentrations during RTE
 1893 is highest among the northern latitudes, it gradually decreased over south. Such aerosol transport has induced
 1894 occurrence of an aerosol layer, referred as TAL, having thickness of ~ 1 -2 km departed from ABL. While the TAL
 1895 has relatively lower vertical extension over the northern latitudes (~ 2 km), it eventually broadens over the southern
 1896 latitudes (~ 3 km). Moreover, occurrence of TAL constituted an atmospheric warming up to ~ 1 -1.5°C where it
 1897 present. The RTE episodes, in general, promotes the lower tropospheric stability and hence suppress the growth
 1898 of ABL. Such inhibition of the ABL growth has a latitudinal heterogeneity. Overall, the occurrence of RTE and
 1899 TAL have suppressed the ABL-H by $\sim 40\%$ and such suppression are dominant during the afternoon hours. Finally,
 1900 the relation between the ABL-H and $PM_{2.5}$ aggravations are delineated. For instance, a 30% reduction in the ABL-
 1901 H can contribute to ~ 130 -150% increase in the surface $PM_{2.5}$ concentrations. The diurnal variation of the $PM_{2.5}$
 1902 suggests an overall enhancement of $\sim 55\%$ during RTE compared to clear day; however, such enhancements are
 1903 dominant between 09-11 LT.

1904 This study elucidates the first qualitative investigation of the transboundary transport of aerosols over the
 1905 Indian peninsula and is a reference for emission policies over the eastern coasts, especially over Chennai and the
 1906 surrounding area. The analysis of the TAL is carried out by removing the cases of shallow clouds occurring
 1907 frequently during the study period, which we would like to pursue in a future study.

- Deleted: T
- Deleted: surface
- Deleted:
- Deleted: 8
- Deleted: 3
- Deleted: 3
- Deleted: 40-45
- Deleted: 20 - 2
- Deleted: 3
- Deleted:
- Formatted ... [97]
- Deleted: Although the clear-day composite shows a ... [98]
- Deleted: 30
- Deleted: $\mu\text{g}/\text{m}^3$ between 08:00 and 15:00 LT,
- Deleted:
- Deleted: it rapidly decreases from 75
- Deleted: 60
- Deleted: $\mu\text{g}/\text{m}^3$ to 36
- Deleted: 32
- Deleted: $\mu\text{g}/\text{m}^3$ during RTE days. As depicted in
- Deleted: 2e
- Deleted: ,
- Deleted: enhancement
- Deleted: 2d, the enhancement
- Deleted: in the aerosol extinction coefficient is minit ... [99]
- Deleted: ¶
- Deleted: Please check the cited papers you have in ... [100]
- Deleted: transboundary
- Deleted: pollution
- Deleted: dispersion
- Formatted ... [101]
- Deleted: is segregated from the spatial distribution ... [102]
- Deleted: ,
- Deleted:),
- Deleted:
- Deleted: influenced
- Deleted: by
- Deleted: formation
- Deleted: over the northern BoB and prevalent north ... [103]
- Deleted: west
- Deleted: and nearby
- Formatted ... [104]
- Formatted ... [105]
- Deleted: ¶

1971 **Data Availability**

1972 MODIS and MERRA2 data can be obtained from NASA Goddard Earth Sciences Data and Information Services

1973 Center (GES DISC). CALIPSO data used in this study can be obtained directly from the website

1974 https://eosweb.larc.nasa.gov/project/calipso/calipso_table. Radiosonde and surface data can be obtained from the

1975 <https://weather.uwyo.edu/upperair/sounding.html>. The MPL data used in this study are not publicly available;

1976 however, the data can be provided to the corresponding author upon request.

1977 Author contributions.

1978 SA was responsible for carrying out the investigation, writing, reviewing, data curation, and preparing the original

1979 draft of the paper. CS is responsible for conceptualizing, methodology and supervising, carrying out the

1980 investigation, writing, reviewing, and editing the paper. SKM is responsible for MPL data curation, reviewing and

1981 editing the paper

1982 Competing interests.

1983 The contact author has declared that neither they nor their co-authors have any competing interests

1984 Acknowledgements

1985 SA thanks the Asia-Pacific Network for Global Change Research (APN) research grant (CRRP2022-08MY-

1986 Sarangi) for supporting this work. CS is grateful to MoES Deep Ocean mission project for the support of

1987 computational facility for this work.

Deleted: ADD, make conclusive paragraphs (crisp 4-5 sentences max) on:¶
The spatial and elevation characteristics of RTE (as seen in Figure 1+2)¶
The observed atmospheric warming, LTS from Radiosonde analysis (Figure 3)¶
The observed ABLH reduction and associated ABLH-PM2.5 enhancement relationship over Chennai (Figure 4+5)coast of BoB and nearby regions.¶
The occurrence of RTE days generally prolongs for more than a day. The largest lapsed RTE were observed during March 2022, which continued for 12 consecutive days. The widespread haziness over the northeastern region of the Indian subcontinent induced by the occurrence of TAL, especially during the winter season, is mainly favoured by the relative reduction of wind speed during the season near the surface. The reduced windspeed declines the dispersion of pollutants over a large area in the southern Indian peninsula hence reducing any diurnal variability in the aerosol distribution. On the other hand, although the overall WS declines during RTE days compared to clear days, it shows some enhancement above ~1.5 km, promoting the formation and growth of TAL aloft the ABL. ¶
The TAL has a ~1-2 km thickness and occurs just above the ABL. A strong temperature inversion between the top of the TAL and free troposphere is observed during the RTE periods, followed by a strong warming up to ~1-1.5°C where the TAL is present, constituting an increment of ~5-10% relative to clear sky days. While the TAL has relatively lower vertical extension over the northern latitudes (~2 km), it eventually broadens over the southern latitudes (~3 km). The RTE episodes, in general, promotes the lower tropospheric stability and hence suppress the growth of ABL. Such inhibition of the ABL growth has a latitudinal variability. Overall, high resolution lidar observations over Chennai suggest that the RTE and occurrence of TAL have suppressed the ABL-H by ~38%; however, for a typical RTE episode, temporal variation in the aerosol extinction characteristic suggests a suppression of up to ~78 %. The occurrence and maintenance of TAL during the RTE are favoured by the strong wind flow from north India, which majorly contributes to the reduction of the ABL-H and aggravation of surface pollution. The aerosol “dome effect”, as a result of the vertical temperature stratification due to the presence of TAL, has induced the suppression of the ABL-H and increased the surface PM2.5 by ~30-35% compared to the clear days. This study elucidates the first qualitative investigation of the transboundary transport of aerosols over the Indian peninsula and is a reference for emission policies over the eastern coasts, especially over Chennai and the surrounding area. The analysis of the TAL is carried out by removing the cases of shallow clouds occurring frequently during the study period, which we would like to pursue in a future study.¶

Formatted: Font: 10 pt

Deleted: the study

Deleted: NET

Deleted: data

Deleted: collection

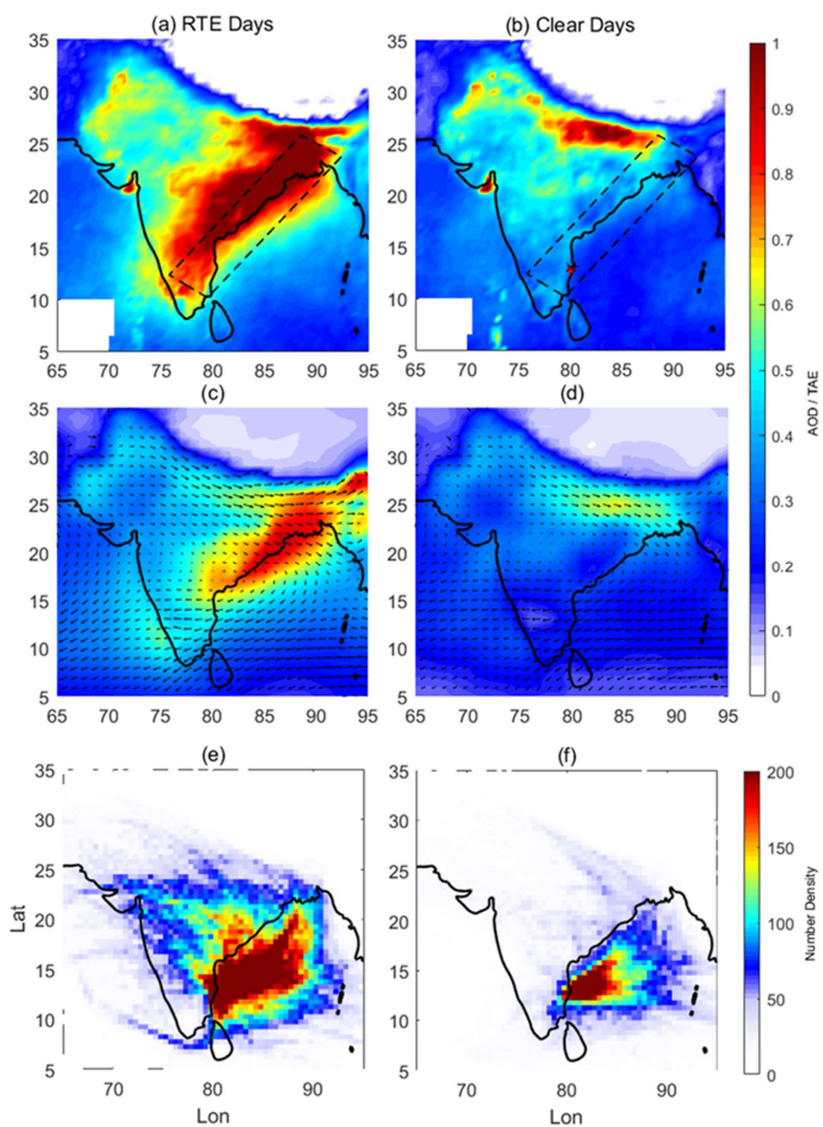
Deleted: ¶

Deleted: ¶

¶

... [106]

2114 Figures.



2115

2116 Figure 1 Composite of the spatial distribution of AOD obtained from MODIS during (a) RTE and (b) clear
 2117 days between December and March during 2015-2024 and total aerosol extinction (TAE) from MERRA2
 2118 reanalysis dataset observed for the composite of (c) RTE and (d) clear days. [Number density of 5-day](#)
 2119 [backward air mass trajectories to Chennai between surface and 4 km during \(e\) RTE and \(f\) Clear days.](#)

2120

Deleted: Panel (e) shows the statistics of occurrence frequency of RTE day periods segregated for 1 day (black), 2-4 days (magenta) and more than 4 days (red). (f) Difference in the wind speed between RTE and clear days at 850 hPa.

2126

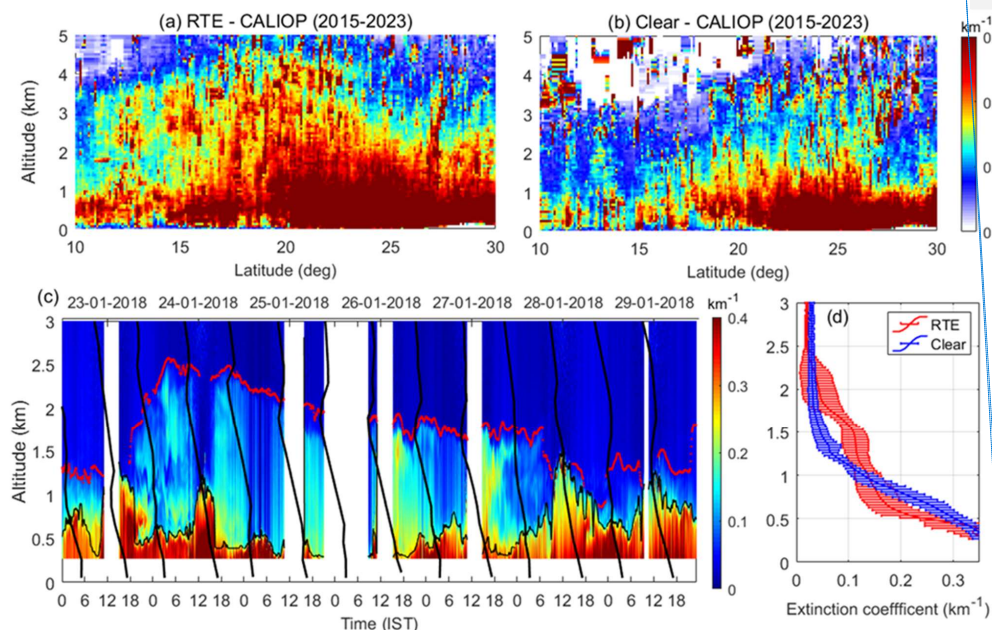
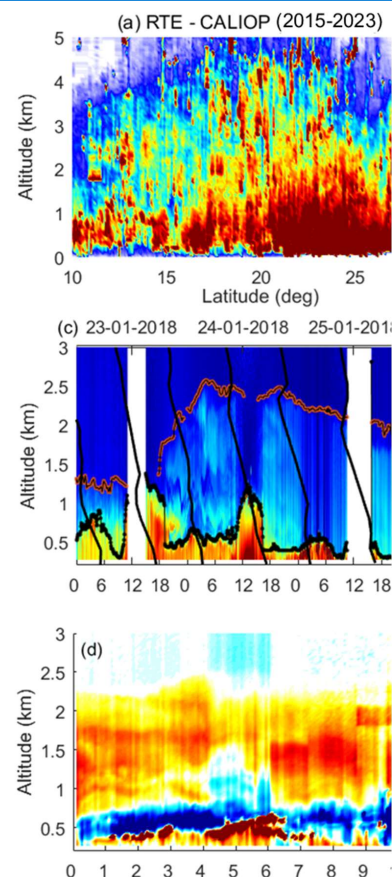


Figure 2. The vertical distribution of the aerosol extinction coefficient from CALIOP during the (a) RTE and (b) clear days within $\pm 5^\circ$ longitude over the eastern coast of India between December and March 2015-2023. (c) Time-Altitude cross-section of the total attenuated extinction coefficient obtained from Micro Pulse Lidar (MPL) observation over Chennai (SRM IST) between 23 and 29 January 2018. The black line corresponds to the temperature profiles from radiosonde over IMD, Chennai. The black dotted line corresponds to the derived ABL-H, and the red dotted lines are the top of the TAL. (d) Mean extinction coefficient observed during a typical RTE (24 - 27 Jan 2018) and clear day (23,28,29 Jan 2018) estimated from MPL observation.



Deleted:

Deleted: ¶

¶

[107]

Formatted: Font: (Default) +Body (Aptos), Not Bold, English (United Kingdom)

Deleted: 4

Deleted: transported aerosol layer

Deleted: The difference between the extinction coefficient observed during RTE and clear day is shown as a dotted line (axis on the top). (e) Temporal changes in the difference between the extinction coefficients during the RTE and clear day composite in 2018. (d) Temporal changes in the mean difference between the extinction coefficients during RTE and clear day composite in 2018. [108]

Formatted: English (India)

Deleted: ¶

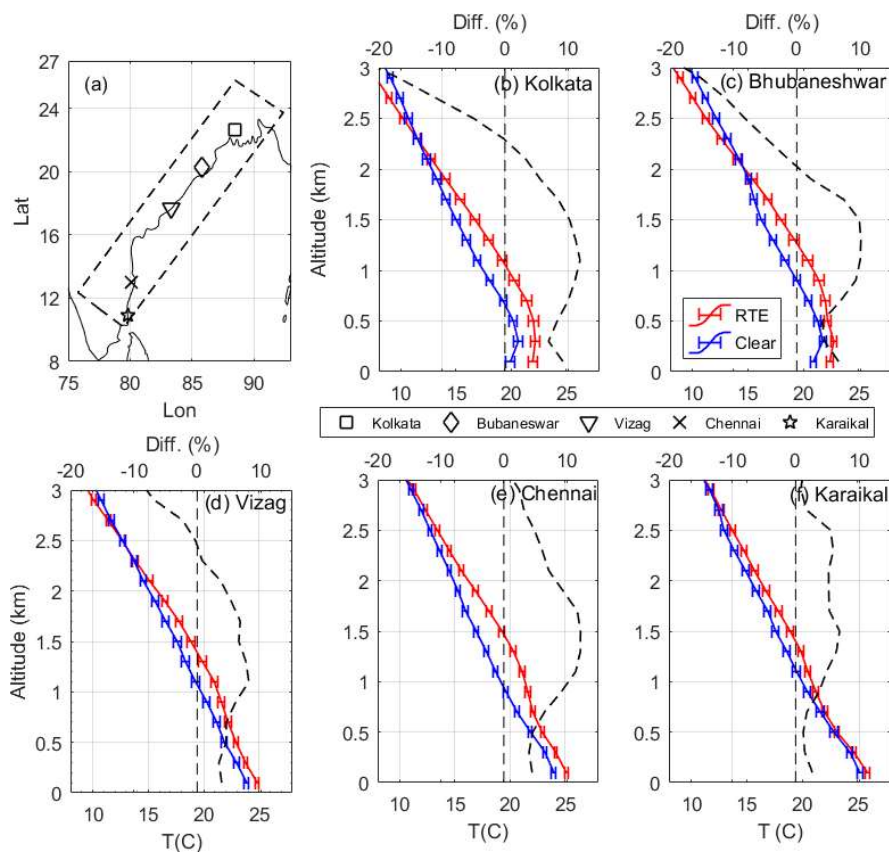
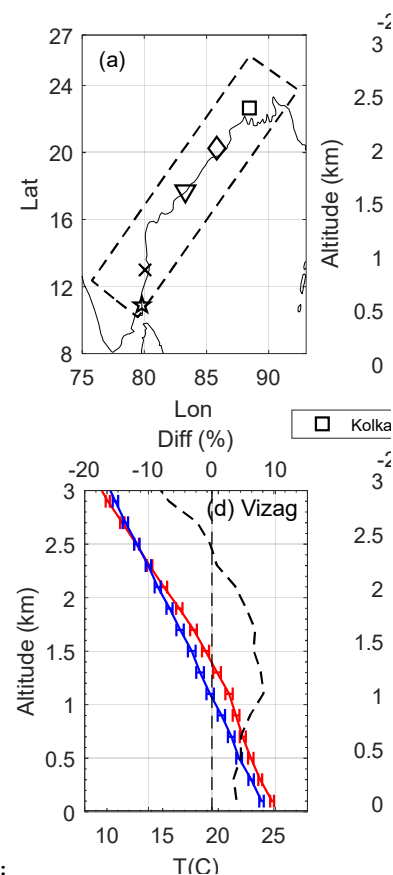


Figure 3 Vertical profiles of temperature during RTE (red) and Clear (blue) days obtained over the different station along the eastern coast. (a) Locations of the Radiosonde observations. (b)-(f) mean temperature profiles with standard errors over the stations Kolkata, Bhubaneswar, Vizag, Chennai and Karaikal during RTE and Clear days, and the difference between the RTE and Clear in percent (axis on the top). Vertical dashed line corresponds to the 0%.



Deleted:

Formatted: Font: 10 pt

Formatted: Font:

Deleted: Vertical variation of Wind Speed (WS), Relative Humidity (RH) and Temperature (T) over Chennai (a-c) and Karaikal (d-f) during RTE (red) and (b) clear days (blue). The difference in the RTE and clear days (RTE-Clear) are shown in dashed line (axes on top). The horizontal bars correspond to the standard errors.

Formatted: Font: English (United Kingdom)

Formatted: Space Before: 12 pt

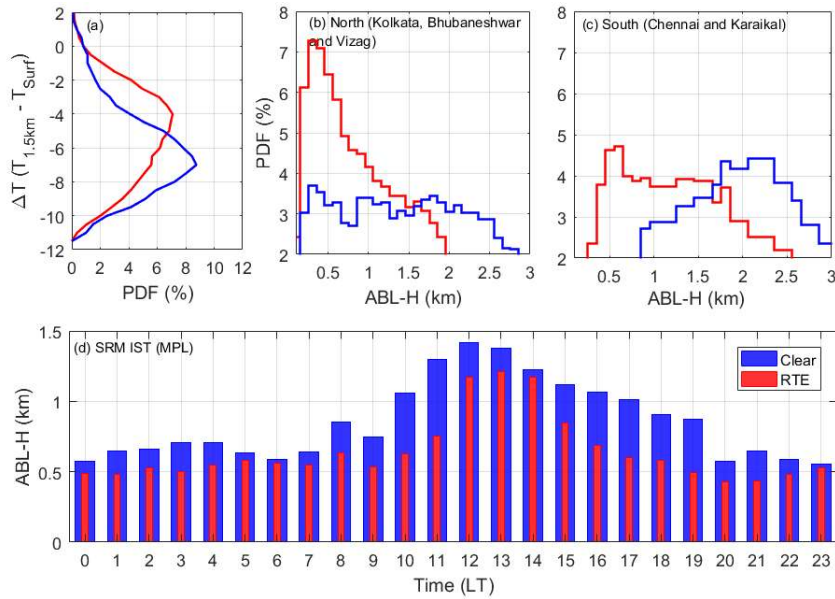
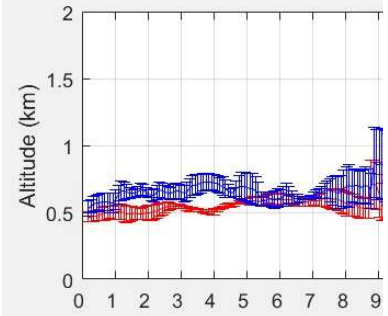


Figure 4. (a) The probability distribution of difference in the temperature between 1.5 km and surface during RTE (red) and clear (blue) days, obtained across all the station over the eastern coast. Probability distribution of ABL-H across (b) the north stations (Kolkata and Bhubaneswar and Vizag, (c) Chennai and Karaikal obtained during RTE (red) and clear(blue) days. (d) Diurnal variation of the mean ABL-H observed over SRM IST from MPL observation during RTE and clear days.



Deleted:

Deleted: <object>

Deleted: ¶

Formatted: Font:

Formatted: Font:

Deleted: ¶

¶

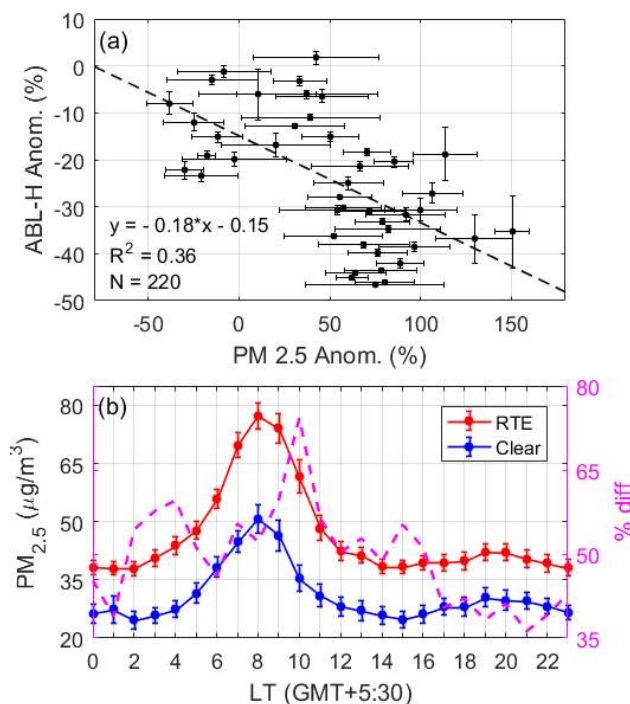
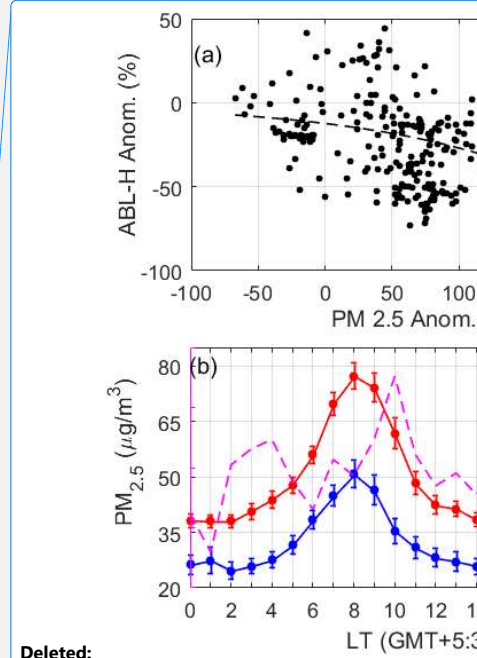


Figure 5. a) Scatter plot showing the normalized anomaly of PM_{2.5} and ABL-H (obtained from MPL, in percent) during the RTE days as observed by MPL. The linear fit, R² and number of samples (N) are also provided. b) Diurnal variation of PM_{2.5} over Chennai (US Consulate, Chennai) during RTE and clear days. The percentage difference in the PM_{2.5} (%diff, magenta color) is shown in right axis.



Deleted:

Deleted: <object>

Deleted: 4. Probability distribution (%) of (a) difference in temperature between 1.5

Deleted: km and surface (ΔT; bin size=2K) and the (

Deleted: b) ABL-H obtained during climatological RTE (red) and clear (blue) cases (bin size=0.2km). (c)

Deleted: PM₂

Deleted: . The red scatters show the cases when wind speed (WS) is exceeds 4 m/s and red circles for the cases where wind directed from north to north east.

Deleted: The correlation coefficient, exponential fit (dashed line) equation, R² and number of samples also provided. (

Deleted: d

Deleted: ¶
¶

- 2238 **References:**
- 2239 Ali, S., Mehta, S. K., Ananthavel, A. and Reddy, T. V. R.: Temporal and vertical distributions of the occurrence
 2240 of cirrus clouds over a coastal station in the Indian monsoon region, *Atmos. Chem. Phys.*, 22(12), 8321–8342,
 2241 doi:10.5194/acp-22-8321-2022, 2022.
- 2242 Ananthavel, A., Mehta, S. K., Ali, S., Reddy, T. V. R., Annamalai, V. and Rao, D. N.: Micro Pulse Lidar
 2243 measurements in coincidence with CALIPSO overpasses: Comparison of tropospheric aerosols over
 2244 Kattankulathur (12.82oN, 80.04oE), *Atmos. Pollut. Res.*, 12(6), 101082, doi:10.1016/j.apr.2021.101082, 2021a.
- 2245 Ananthavel, A., Mehta, S. K., Reddy, T. V. R., Ali, S. and Rao, D. N.: Vertical distributions and columnar
 2246 properties of the aerosols during different seasons over Kattankulathur (12.82oN, 80.04oE): A semi-urban
 2247 tropical coastal station, *Atmos. Environ.*, 256, 118457, doi:10.1016/j.atmosenv.2021.118457, 2021b.
- 2248 Aruna, K., Kumar, T. V. L., Rao, D. N., Murthy, B. V. K., Babu, S. S. and Moorthy, K. K.: Black carbon
 2249 aerosols in a tropical semi-urban coastal environment: Effects of boundary layer dynamics and long range
 2250 transport, *J. Atmos. Solar-Terrestrial Phys.*, 104, 116–125, doi:10.1016/j.jastp.2013.08.020, 2013.
- 2251 Baars, H., Ansmann, A., Engelmann, R. and Althausen, D.: Continuous monitoring of the boundary-layer top
 2252 with lidar, *Atmos. Chem. Phys.*, 8(23), 7281–7296, doi:10.5194/acp-8-7281-2008, 2008.
- 2253 Barbaro, E., de Arellano, J. V., Ouwersloot, H. G., Schröter, J. S., Donovan, D. P. and Krol, M. C.: Aerosols in
 2254 the convective boundary layer: Shortwave radiation effects on the coupled land-atmosphere system, *J. Geophys.*
 2255 *Res. Atmos.*, 119(10), 5845–5863, doi:10.1002/2013JD021237, 2014.
- 2256 Chester, R., Berry, A. S. and Murphy, K. J. T.: The distributions of particulate atmospheric trace metals and
 2257 mineral aerosols over the Indian Ocean, *Mar. Chem.*, 34(3–4), 261–290, doi:10.1016/0304-4203(91)90007-J,
 2258 1991.
- 2259 Comstock, J. M. and Sassen, K.: Retrieval of cirrus cloud radiative and backscattering properties using
 2260 combined lidar and infrared radiometer (LIRAD) measurements, *J. Atmos. Ocean. Technol.*, 18(10), 1658–
 2261 1673, doi:10.1175/1520-0426(2001)018<1658:ROCCRA>2.0.CO;2, 2001.
- 2262 Dagan, G. and Eytan, E.: The Potential of Absorbing Aerosols to Enhance Extreme Precipitation, *Geophys. Res.*
 2263 *Lett.*, 51(10), doi:10.1029/2024GL108385, 2024.
- 2264 Davis, K. J., Gamage, N., Hagelberg, C. R., Kiemle, C., Lenschow, D. H. and Sullivan, P. P.: An Objective
 2265 Method for Deriving Atmospheric Structure from Airborne Lidar Observations, *J. Atmos. Ocean. Technol.*,
 2266 17(11), 1455–1468, doi:10.1175/1520-0426(2000)017<1455:AOMFDA>2.0.CO;2, 2000.
- 2267 Ding, A. J., Fu, C. B., Yang, X. Q., Sun, J. N., Petäjä, T., Kerminen, V.-M., Wang, T., Xie, Y., Herrmann, E.,
 2268 Zheng, L. F., Nie, W., Liu, Q., Wei, X. L. and Kulmala, M.: Intense atmospheric pollution modifies weather: a
 2269 case of mixed biomass burning with fossil fuel combustion pollution in eastern China, *Atmos. Chem. Phys.*,
 2270 13(20), 10545–10554, doi:10.5194/acp-13-10545-2013, 2013.
- 2271 Ding, A. J., Huang, X., Nie, W., Sun, J. N., Kerminen, V. -M., Petäjä, T., Su, H., Cheng, Y. F., Yang, X. -Q.,
 2272 Wang, M. H., Chi, X. G., Wang, J. P., Virkkula, A., Guo, W. D., Yuan, J., Wang, S. Y., Zhang, R. J., Wu, Y. F.,
 2273 Song, Y., Zhu, T., Zilitinkevich, S., Kulmala, M. and Fu, C. B.: Enhanced haze pollution by black carbon in
 2274 megacities in China, *Geophys. Res. Lett.*, 43(6), 2873–2879, doi:10.1002/2016GL067745, 2016.
- 2275 Dipu, S., Prabha, T. V., Pandithurai, G., Dudhia, J., Pfister, G., Rajesh, K. and Goswami, B. N.: Impact of
 2276 elevated aerosol layer on the cloud macrophysical properties prior to monsoon onset, *Atmos. Environ.*, 70, 454–
 2277 467, doi:10.1016/j.atmosenv.2012.12.036, 2013.
- 2278 Garratt, J.: Review: the atmospheric boundary layer, *Earth-Science Rev.*, 37(1–2), 89–134, doi:10.1016/0012-
 2279 8252(94)90026-4, 1994.
- 2280 Gelaro, R., McCarty, W., Suárez, M. J., Todling, R., Molod, A., Takacs, L., Randles, C. A., Darmenov, A.,
 2281 Bosilovich, M. G., Reichle, R., Wargan, K., Coy, L., Cullather, R., Draper, C., Akella, S., Buchard, V., Conaty,
 2282 A., da Silva, A. M., Gu, W., Kim, G.-K., Koster, R., Lucchesi, R., Merkova, D., Nielsen, J. E., Partyka, G.,
 2283 Pawson, S., Putman, W., Rienecker, M., Schubert, S. D., Sienkiewicz, M. and Zhao, B.: The Modern-Era
 2284 Retrospective Analysis for Research and Applications, Version 2 (MERRA-2), *J. Clim.*, 30(14), 5419–5454,
 2285 doi:10.1175/JCLI-D-16-0758.1, 2017.
- 2286 Guo, J., Xia, F., Zhang, Y., Liu, H., Li, J., Lou, M., He, J., Yan, Y., Wang, F., Min, M. and Zhai, P.: Impact of

Deleted: ¶



2291 diurnal variability and meteorological factors on the PM_{2.5} - AOD relationship: Implications for PM_{2.5} remote
2292 sensing, *Environ. Pollut.*, 221, 94–104, doi:10.1016/j.envpol.2016.11.043, 2017.

2293 Guo, S., Hu, M., Zamora, M. L., Peng, J., Shang, D., Zheng, J., Du, Z., Wu, Z., Shao, M., Zeng, L., Molina, M.
2294 J. and Zhang, R.: Elucidating severe urban haze formation in China, *Proc. Natl. Acad. Sci.*, 111(49), 17373–
2295 17378, doi:10.1073/pnas.1419604111, 2014.

2296 Haywood, J. and Boucher, O.: Estimates of the direct and indirect radiative forcing due to tropospheric aerosols:
2297 A review, *Rev. Geophys.*, 38(4), 513–543, doi:10.1029/1999RG000078, 2000.

2298 Huang, J., Minnis, P., Yi, Y., Tang, Q., Wang, X., Hu, Y., Liu, Z., Ayers, K., Trepte, C. and Winker, D.:
2299 Summer dust aerosols detected from CALIPSO over the Tibetan Plateau, *Geophys. Res. Lett.*, 34(18),
2300 doi:10.1029/2007GL029938, 2007.

2301 Huang, X., Wang, Z. and Ding, A.: Impact of Aerosol-PBL Interaction on Haze Pollution: Multiyear
2302 Observational Evidences in North China, *Geophys. Res. Lett.*, 45(16), 8596–8603, doi:10.1029/2018GL079239,
2303 2018.

2304 Jiang, J., Zhou, W., Cheng, Z., Wang, S., He, K. and Hao, J.: Particulate Matter Distributions in China during a
2305 Winter Period with Frequent Pollution Episodes (January 2013), *Aerosol Air Qual. Res.*, 15(2), 494–503,
2306 doi:10.4209/aaqr.2014.04.0070, 2015.

2307 Kakkannattu, S. P., Mehta, S. K., Purushotham, P., Betsy, K. B., Seetha, C. J. and Musaid, P. P.: Continuous
2308 monitoring of the atmospheric boundary layer (ABL) height from micro pulse lidar over a tropical coastal
2309 station, Kattankulathur (12.82° N, 80.04° E), *Meteorol. Atmos. Phys.*, 135(1), 2, doi:10.1007/s00703-022-
2310 00938-x, 2023.

2311 Kant, S., Sarangi, C. and Wilcox, E. M.: Aerosol processes perturb cloud trends over Bay of Bengal:
2312 observational evidence, *npj Clim. Atmos. Sci.*, 6(1), 132, doi:10.1038/s41612-023-00443-x, 2023.

2313 Kaufman, Y. J., Wald, A. E., Remer, L. A., Bo-Cai Gao, Rong-Rong Li and Flynn, L.: The MODIS 2.1- μ m
2314 channel-correlation with visible reflectance for use in remote sensing of aerosol, *IEEE Trans. Geosci. Remote*
2315 *Sens.*, 35(5), 1286–1298, doi:10.1109/36.628795, 1997.

2316 Krishnamurti, T. N., Jha, B., Prospero, J., Jayaraman, A. and Ramanathan, V.: Aerosol and pollutant transport
2317 and their impact on radiative forcing over the tropical Indian Ocean during the January–February 1996 pre-
2318 INDOEX cruise, *Tellus B Chem. Phys. Meteorol.*, 50(5), 521, doi:10.3402/tellusb.v50i5.16235, 1998.

2319 Li, Z., Guo, J., Ding, A., Liao, H., Liu, J., Sun, Y., Wang, T., Xue, H., Zhang, H. and Zhu, B.: Aerosol and
2320 boundary-layer interactions and impact on air quality, *Natl. Sci. Rev.*, 4(6), 810–833, doi:10.1093/nsr/nwx117,
2321 2017.

2322 Liu, G., Xin, J., Wang, X., Si, R., Ma, Y., Wen, T., Zhao, L., Zhao, D., Wang, Y. and Gao, W.: Impact of the
2323 coal banning zone on visibility in the Beijing-Tianjin-Hebei region, *Sci. Total Environ.*, 692, 402–410,
2324 doi:10.1016/j.scitotenv.2019.07.006, 2019.

2325 Lohmann, U. and Feichter, J.: Global indirect aerosol effects: a review, *Atmos. Chem. Phys.*, 5(3), 715–737,
2326 doi:10.5194/acp-5-715-2005, 2005.

2327 Lyapustin, A., Wang, Y., Laszlo, I., Kahn, R., Korkin, S., Remer, L., Levy, R. and Reid, J. S.: Multiangle
2328 implementation of atmospheric correction (MAIAC): 2. Aerosol algorithm, *J. Geophys. Res.*, 116(D3), D03211,
2329 doi:10.1029/2010JD014986, 2011a.

2330 Lyapustin, A., Smirnov, A., Holben, B., Chin, M., Streets, D. G., Lu, Z., Kahn, R., Slutsker, I., Laszlo, I.,
2331 Kondragunta, S., Tanré, D., Dubovik, O., Goloub, P., Chen, H.-B., Sinyuk, A., Wang, Y. and Korkin, S.:
2332 Reduction of aerosol absorption in Beijing since 2007 from MODIS and AERONET, *Geophys. Res. Lett.*,
2333 38(10), n/a-n/a, doi:10.1029/2011GL047306, 2011b.

2334 Ma, Y., Ye, J., Xin, J., Zhang, W., Vilà-Guerau de Arellano, J., Wang, S., Zhao, D., Dai, L., Ma, Y., Wu, X.,
2335 Xia, X., Tang, G., Wang, Y., Shen, P., Lei, Y. and Martin, S. T.: The Stove, Dome, and Umbrella Effects of
2336 Atmospheric Aerosol on the Development of the Planetary Boundary Layer in Hazy Regions, *Geophys. Res.*
2337 *Lett.*, 47(13), doi:10.1029/2020GL087373, 2020.

2338 Ma, Y., Xin, J., Wang, Z., Tian, Y., Wu, L., Tang, G., Zhang, W., de Arellano, J. V.-G., Zhao, D., Jia, D., Ren,
2339 Y., Gao, Z., Shen, P., Ye, J. and Martin, S. T.: How do aerosols above the residual layer affect the planetary

2340 boundary layer height?, *Sci. Total Environ.*, 814, 151953, doi:10.1016/j.scitotenv.2021.151953, 2022.

2341 Mehta, S. K., Ojha, D., Mehta, S., Anand, D., Rao, D. N., Annamalai, V., Ananthavel, A. and Ali, S.:
2342 Thermodynamic structure of the convective boundary layer (CBL) over the Indian monsoon region during
2343 CAIPEEX campaigns, , (iv), 1361–1379, 2017.

2344 Mehta, S. K., Ananthavel, A., Velu, V., Prabhakaran, T., Pandithurai, G. and Rao, D. N.: Characteristics of
2345 elevated aerosol layer over the Indian east coast, Kattankulathur (12.82oN, 80.04°E): A northeast monsoon
2346 region, *Sci. Total Environ.*, 886, 163917, doi:10.1016/j.scitotenv.2023.163917, 2023.

2347 Mhawish, A., Sarangi, C., Babu, P., Kumar, M., Bilal, M. and Qiu, Z.: Observational evidence of elevated
2348 smoke layers during crop residue burning season over Delhi: Potential implications on associated heterogeneous
2349 PM_{2.5} enhancements, *Remote Sens. Environ.*, 280, 113167, doi:10.1016/j.rse.2022.113167, 2022.

2350 Miao, Y. and Liu, S.: Linkages between aerosol pollution and planetary boundary layer structure in China, *Sci.*
2351 *Total Environ.*, 650, 288–296, doi:10.1016/j.scitotenv.2018.09.032, 2019.

2352 Mukherjee, A. and Toohey, D. W.: A study of aerosol properties based on observations of particulate matter
2353 from the U.S. Embassy in Beijing, China, *Earth's Futur.*, 4(8), 381–395, doi:10.1002/2016EF000367, 2016.

2354 Pal, S., Behrendt, A. and Wulfmeyer, V.: Elastic-backscatter-lidar-based characterization of the convective
2355 boundary layer and investigation of related statistics, *Ann. Geophys.*, 28(3), 825–847, doi:10.5194/angeo-28-
2356 825-2010, 2010.

2357 Petäjä, T., Järvi, L., Kerminen, V.-M., Ding, A. J., Sun, J. N., Nie, W., Kujansuu, J., Virkkula, A., Yang, X., Fu,
2358 C. B., Zilitinkevich, S. and Kulmala, M.: Enhanced air pollution via aerosol-boundary layer feedback in China,
2359 *Sci. Rep.*, 6(1), 18998, doi:10.1038/srep18998, 2016.

2360 Prasad, A. K., Singh, R. P. and Kafatos, M.: Influence of coal based thermal power plants on aerosol optical
2361 properties in the Indo-Gangetic basin, *Geophys. Res. Lett.*, 33(5), doi:10.1029/2005GL023801, 2006.

2362 Prijith, S. S., Rao, P. V. N. and Mohan, M.: Genesis of elevated aerosol loading over the Indian region, edited
2363 by T. N. Krishnamurti and M. N. Rajeevan, p. 988208., 2016.

2364 Prodi, F., Santachiara, G. and Oliosi, F.: Characterization of aerosols in marine environments (Mediterranean,
2365 Red Sea, and Indian Ocean), *J. Geophys. Res. Ocean.*, 88(C15), 10957–10968, doi:10.1029/JC088iC15p10957,
2366 1983.

2367 Qin, K., Wu, L., Wong, M. S., Letu, H., Hu, M., Lang, H., Sheng, S., Teng, J., Xiao, X. and Yuan, L.: Trans-
2368 boundary aerosol transport during a winter haze episode in China revealed by ground-based Lidar and
2369 CALIPSO satellite, *Atmos. Environ.*, 141, 20–29, doi:10.1016/j.atmosenv.2016.06.042, 2016.

2370 Quan, J., Gao, Y., Zhang, Q., Tie, X., Cao, J., Han, S., Meng, J., Chen, P. and Zhao, D.: Evolution of planetary
2371 boundary layer under different weather conditions, and its impact on aerosol concentrations, *Particuology*,
2372 11(1), 34–40, doi:10.1016/j.partic.2012.04.005, 2013.

2373 Quan, J., Tie, X., Zhang, Q., Liu, Q., Li, X., Gao, Y. and Zhao, D.: Characteristics of heavy aerosol pollution
2374 during the 2012–2013 winter in Beijing, China, *Atmos. Environ.*, 88, 83–89,
2375 doi:10.1016/j.atmosenv.2014.01.058, 2014.

2376 Raatikainen, T., Hyvärinen, A.-P., Hatakka, J., Panwar, T. S., Hooda, R. K., Sharma, V. P. and Lihavainen, H.:
2377 The effect of boundary layer dynamics on aerosol properties at the Indo-Gangetic plains and at the foothills of
2378 the Himalayas, *Atmos. Environ.*, 89, 548–555, doi:10.1016/j.atmosenv.2014.02.058, 2014.

2379 Rajeev, K., Ramanathan, V. and Meywerk, J.: Regional aerosol distribution and its long-range transport over the
2380 Indian Ocean, *J. Geophys. Res. Atmos.*, 105(D2), 2029–2043, doi:10.1029/1999JD900414, 2000.

2381 Rajeevan, M. and Srinivasan, J.: Net Cloud Radiative Forcing at the Top of the Atmosphere in the Asian
2382 Monsoon Region, *J. Clim.*, 13(3), 650–657, doi:10.1175/1520-0442(2000)013<0650:NCRFAT>2.0.CO;2, 2000.

2383 Ramanathan, V., Crutzen, P. J., Coakley, J., Dickerson, R., Heymsfield, A., Kiehl, J., Kley, D., Krishnamurti,
2384 T. N., Kuettner, J., Lelieveld, J. and Mitra, A. P.: Indian Ocean Experiment (INDOEX) White Paper, C4 Publ,
2385 143, 1995.

2386 Ramanathan, V. and Ramana, M. V.: Persistent, Widespread, and Strongly Absorbing Haze Over the Himalayan
2387 Foothills and the Indo-Gangetic Plains, *Pure Appl. Geophys.*, 162(8–9), 1609–1626, doi:10.1007/s00024-005-

2388 2685-8, 2005.

2389 Ramanathan, V., Crutzen, P. J., Kiehl, J. T. and Rosenfeld, D.: Aerosols, Climate, and the Hydrological Cycle,
2390 Science (80-.), 294(5549), 2119–2124, doi:10.1126/science.1064034, 2001.

2391 Randles, C. A., da Silva, A. M., Buchard, V., Colarco, P. R., Darmenov, A., Govindaraju, R., Smirnov, A.,
2392 Holben, B., Ferrare, R., Hair, J., Shinozuka, Y. and Flynn, C. J.: The MERRA-2 Aerosol Reanalysis, 1980
2393 Onward. Part I: System Description and Data Assimilation Evaluation, J. Clim., 30(17), 6823–6850,
2394 doi:10.1175/JCLI-D-16-0609.1, 2017.

2395 Ratnam, M. V., Prasad, P., Roja Raman, M., Ravikiran, V., Bhaskara Rao, S. V., Krishna Murthy, B. V. and
2396 Jayaraman, A.: Role of dynamics on the formation and maintenance of the elevated aerosol layer during
2397 monsoon season over south-east peninsular India, Atmos. Environ., 188, 43–49,
2398 doi:10.1016/j.atmosenv.2018.06.023, 2018.

2399 Reddy, T. V. R., Mehta, S. K., Ananthavel, A., Ali, S. and Rao, D. N.: Evolution of the planetary boundary
2400 layer and its simulation over a tropical coastal station Kattankulathur (12.83°N, 80.04°E), Theor. Appl.
2401 Climatol., 146(3–4), 1043–1060, doi:10.1007/s00704-021-03770-2, 2021a.

2402 Reddy, T. V. R., Mehta, S. K., Ananthavel, A., Ali, S., Annamalai, V. and Rao, D. N.: Seasonal characteristics
2403 of sea breeze and thermal internal boundary layer over Indian east coast region, Meteorol. Atmos. Phys., 133(2),
2404 217–232, doi:10.1007/s00703-020-00746-1, 2021b.

2405 Rolph, G., Stein, A. and Stunder, B.: Real-time Environmental Applications and Display sYstem: READY,
2406 Environ. Model. Softw., 95, 210–228, doi:10.1016/j.envsoft.2017.06.025, 2017.

2407 Sarangi, C., Kanawade, V. P., Tripathi, S. N., Thomas, A. and Ganguly, D.: Aerosol-induced intensification of
2408 cooling effect of clouds during Indian summer monsoon, Nat. Commun., 9(1), 3754, doi:10.1038/s41467-018-
2409 06015-5, 2018.

2410 SATHEESH, S. and KRISHNAMOORTHY, K.: Radiative effects of natural aerosols: A review, Atmos.
2411 Environ., 39(11), 2089–2110, doi:10.1016/j.atmosenv.2004.12.029, 2005.

2412 Savoie, D. L., Prospero, J. M. and Saltzman, E. S.: Non-sea-salt sulfate and nitrate in trade wind aerosols at
2413 Barbados: Evidence for long-range transport, J. Geophys. Res. Atmos., 94(D4), 5069–5080,
2414 doi:10.1029/JD094iD04p05069, 1989.

2415 Shi, Y., Liu, B., Chen, S., Gong, W., Ma, Y., Zhang, M., Jin, S. and Jin, Y.: Characteristics of aerosol within the
2416 nocturnal residual layer and its effects on surface PM_{2.5} over China, Atmos. Environ., 241, 117841,
2417 doi:10.1016/j.atmosenv.2020.117841, 2020.

2418 Stein, A. F., Draxler, R. R., Rolph, G. D., Stunder, B. J. B., Cohen, M. D. and Ngan, F.: NOAA’s HYSPLIT
2419 Atmospheric Transport and Dispersion Modeling System, Bull. Am. Meteorol. Soc., 96(12), 2059–2077,
2420 doi:10.1175/BAMS-D-14-00110.1, 2015.

2421 Stohl, A.: Characteristics of atmospheric transport into the Arctic troposphere, J. Geophys. Res. Atmos.,
2422 111(D11), doi:10.1029/2005JD006888, 2006.

2423 Stull, R.: An introduction to boundary layer meteorology., 1988.

2424 Sun, X., Zhou, Y., Zhao, T., Fu, W., Wang, Z., Shi, C., Zhang, H., Zhang, Y., Yang, Q. and Shu, Z.: Vertical
2425 distribution of aerosols and association with atmospheric boundary layer structures during regional aerosol
2426 transport over central China, Environ. Pollut., 362, 124967, doi:10.1016/j.envpol.2024.124967, 2024.

2427 Thomas, A., Sarangi, C. and Kanawade, V. P.: Recent Increase in Winter Hazy Days over Central India and the
2428 Arabian Sea, Sci. Rep., 9(1), 17406, doi:10.1038/s41598-019-53630-3, 2019.

2429 Thomas, A., Kanawade, V. P., Sarangi, C. and Srivastava, A. K.: Effect of COVID-19 shutdown on aerosol
2430 direct radiative forcing over the Indo-Gangetic Plain outflow region of the Bay of Bengal, Sci. Total Environ.,
2431 782, 146918, doi:10.1016/j.scitotenv.2021.146918, 2021.

2432 Tripathi, S. N., Tare, V., Chinnam, N., Srivastava, A. K., Dey, S., Agarwal, A., Kishore, S., Lal, R. B., Manar,
2433 M., Kanawade, V. P., Chauhan, S. S. S., Sharma, M., Reddy, R. R., Gopal, K. R., Narasimhulu, K., Reddy, L. S.
2434 S., Gupta, S. and Lal, S.: Measurements of atmospheric parameters during Indian Space Research Organization
2435 Geosphere Biosphere Programme Land Campaign II at a typical location in the Ganga basin: 1. Physical and

optical properties, *J. Geophys. Res. Atmos.*, 111(D23), doi:10.1029/2006JD007278, 2006.

Wang, H., Shi, G. Y., Zhang, X. Y., Gong, S. L., Tan, S. C., Chen, B., Che, H. Z. and Li, T.: Mesoscale modelling study of the interactions between aerosols and PBL meteorology during a haze episode in China Jing-Jin-Ji and its near surrounding region – Part 2: Aerosols' radiative feedback effects, *Atmos. Chem. Phys.*, 15(6), 3277–3287, doi:10.5194/acp-15-3277-2015, 2015.

Wang, H., Li, Z., Lv, Y., Xu, H., Li, K., Li, D., Hou, W., Zheng, F., Wei, Y. and Ge, B.: Observational study of aerosol-induced impact on planetary boundary layer based on lidar and sunphotometer in Beijing, *Environ. Pollut.*, 252, 897–906, doi:10.1016/j.envpol.2019.05.070, 2019a.

Wang, Y., Yao, L., Wang, L., Liu, Z., Ji, D., Tang, G., Zhang, J., Sun, Y., Hu, B. and Xin, J.: Mechanism for the formation of the January 2013 heavy haze pollution episode over central and eastern China, *Sci. China Earth Sci.*, 57(1), 14–25, doi:10.1007/s11430-013-4773-4, 2014.

Wang, Y., Wang, Y., Wang, L., Petäjä, T., Zha, Q., Gong, C., Li, S., Pan, Y., Hu, B., Xin, J. and Kulmala, M.: Increased inorganic aerosol fraction contributes to air pollution and haze in China, *Atmos. Chem. Phys.*, 19(9), 5881–5888, doi:10.5194/acp-19-5881-2019, 2019b.

Wang, Y., Yu, M., Wang, Y., Tang, G., Song, T., Zhou, P., Liu, Z., Hu, B., Ji, D., Wang, L., Zhu, X., Yan, C., Ehn, M., Gao, W., Pan, Y., Xin, J., Sun, Y., Kerminen, V.-M., Kulmala, M. and Petäjä, T.: Rapid formation of intense haze episodes via aerosol–boundary layer feedback in Beijing, *Atmos. Chem. Phys.*, 20(1), 45–53, doi:10.5194/acp-20-45-2020, 2020.

Wang, Z., Huang, X. and Ding, A.: Dome effect of black carbon and its key influencing factors: a one-dimensional modelling study, *Atmos. Chem. Phys.*, 18(4), 2821–2834, doi:10.5194/acp-18-2821-2018, 2018.

Wilcox, E. M., Thomas, R. M., Praveen, P. S., Pistone, K., Bender, F. A.-M. and Ramanathan, V.: Black carbon solar absorption suppresses turbulence in the atmospheric boundary layer, *Proc. Natl. Acad. Sci.*, 113(42), 11794–11799, doi:10.1073/pnas.1525746113, 2016.

Winker, D. M., Vaughan, M. A., Omar, A., Hu, Y., Powell, K. A., Liu, Z., Hunt, W. H. and Young, S. A.: Overview of the CALIPSO Mission and CALIOP Data Processing Algorithms, *J. Atmos. Ocean. Technol.*, 26(11), 2310–2323, doi:10.1175/2009JTECHA1281.1, 2009.

Xiang, Y., Zhang, T., Liu, J., Lv, L., Dong, Y. and Chen, Z.: Atmosphere boundary layer height and its effect on air pollutants in Beijing during winter heavy pollution, *Atmos. Res.*, 215, 305–316, doi:10.1016/j.atmosres.2018.09.014, 2019.

Yang, X., Zhao, C., Guo, J. and Wang, Y.: Intensification of aerosol pollution associated with its feedback with surface solar radiation and winds in Beijing, *J. Geophys. Res. Atmos.*, 121(8), 4093–4099, doi:10.1002/2015JD024645, 2016.

Yang, Y., Zheng, Z., Yim, S. Y. L., Roth, M., Ren, G., Gao, Z., Wang, T., Li, Q., Shi, C., Ning, G. and Li, Y.: PM 2.5 Pollution Modulates Wintertime Urban Heat Island Intensity in the Beijing-Tianjin-Hebei Megalopolis, China, *Geophys. Res. Lett.*, 47(1), doi:10.1029/2019GL084288, 2020.

Ye, X., Song, Y., Cai, X. and Zhang, H.: Study on the synoptic flow patterns and boundary layer process of the severe haze events over the North China Plain in January 2013, *Atmos. Environ.*, 124, 129–145, doi:10.1016/j.atmosenv.2015.06.011, 2016.

Young, S. A., Vaughan, M. A., Kuehn, R. E. and Winker, D. M.: The retrieval of profiles of particulate extinction from Cloud-Aerosol Lidar and Infrared Pathfinder Satellite Observations (CALIPSO) data: Uncertainty and error sensitivity analyses, *J. Atmos. Ocean. Technol.*, 30(3), 395–428, doi:10.1175/JTECH-D-12-00046.1, 2013.

Yu, C., Zhao, T., Bai, Y., Zhang, L., Kong, S., Yu, X., He, J., Cui, C., Yang, J., You, Y., Ma, G., Wu, M. and Chang, J.: Heavy air pollution with a unique “non-stagnant” atmospheric boundary layer in the Yangtze River middle basin aggravated by regional transport of PM_{2.5} over China, *Atmos. Chem. Phys.*, 20(12), 7217–7230, doi:10.5194/acp-20-7217-2020, 2020.

Yu, H., Kaufman, Y. J., Chin, M., Feingold, G., Remer, L. A., Anderson, T. L., Balkanski, Y., Bellouin, N., Boucher, O., Christopher, S., DeCola, P., Kahn, R., Koch, D., Loeb, N., Reddy, M. S., Schulz, M., Takemura, T. and Zhou, M.: A review of measurement-based assessments of the aerosol direct radiative effect and forcing, *Atmos. Chem. Phys.*, 6(3), 613–666, doi:10.5194/acp-6-613-2006, 2006.

2486 Yu, H., Remer, L. A., Chin, M., Bian, H., Tan, Q., Yuan, T. and Zhang, Y.: Aerosols from Overseas Rival
2487 Domestic Emissions over North America, *Science* (80-.), 337(6094), 566–569, doi:10.1126/science.1217576,
2488 2012.

2489 Zhang, H., Wang, Y., Hu, J., Ying, Q. and Hu, X.-M.: Relationships between meteorological parameters and
2490 criteria air pollutants in three megacities in China, *Environ. Res.*, 140, 242–254,
2491 doi:10.1016/j.envres.2015.04.004, 2015.

2492 Zhang, M., Tian, P., Zeng, H., Wang, L., Liang, J., Cao, X. and Zhang, L.: A Comparison of Wintertime
2493 Atmospheric Boundary Layer Heights Determined by Tethered Balloon Soundings and Lidar at the Site of
2494 SACOL, *Remote Sens.*, 13(9), 1781, doi:10.3390/rs13091781, 2021a.

2495 Zhang, Y., Zhang, Y., Yu, C. and Yi, F.: Evolution of Aerosols in the Atmospheric Boundary Layer and
2496 Elevated Layers during a Severe, Persistent Haze Episode in a Central China Megacity, *Atmosphere* (Basel).,
2497 12(2), 152, doi:10.3390/atmos12020152, 2021b.

2498 Zhao, D., Xin, J., Gong, C., Quan, J., Liu, G., Zhao, W., Wang, Y., Liu, Z. and Song, T.: The formation
2499 mechanism of air pollution episodes in Beijing city: Insights into the measured feedback between aerosol
2500 radiative forcing and the atmospheric boundary layer stability, *Sci. Total Environ.*, 692, 371–381,
2501 doi:10.1016/j.scitotenv.2019.07.255, 2019.

2502 Zou, J., Sun, J., Ding, A., Wang, M., Guo, W. and Fu, C.: Observation-based estimation of aerosol-induced
2503 reduction of planetary boundary layer height, *Adv. Atmos. Sci.*, 34(9), 1057–1068, doi:10.1007/s00376-016-
2504 6259-8, 2017.

2505
|

Formatted: Line spacing: single, No widow/orphan control, Don't adjust space between Latin and Asian text, Don't adjust space between Asian text and numbers

Page 1: [1] Deleted Chandan Sarangi 06/04/2025 08:48:00

Page 1: [1] Deleted Chandan Sarangi 06/04/2025 08:48:00

Page 1: [1] Deleted Chandan Sarangi 06/04/2025 08:48:00

Page 1: [1] Deleted Chandan Sarangi 06/04/2025 08:48:00

Page 1: [1] Deleted Chandan Sarangi 06/04/2025 08:48:00

Page 1: [2] Deleted Chandan Sarangi 11/04/2025 08:36:00

Page 1: [2] Deleted Chandan Sarangi 11/04/2025 08:36:00

Page 1: [2] Deleted Chandan Sarangi 11/04/2025 08:36:00

Page 1: [2] Deleted Chandan Sarangi 11/04/2025 08:36:00

Page 1: [2] Deleted Chandan Sarangi 11/04/2025 08:36:00

Page 1: [2] Deleted Chandan Sarangi 11/04/2025 08:36:00

Page 1: [2] Deleted Chandan Sarangi 11/04/2025 08:36:00

Page 1: [2] Deleted Chandan Sarangi 11/04/2025 08:36:00

Page 1: [2] Deleted Chandan Sarangi 11/04/2025 08:36:00

Page 1: [2] Deleted Chandan Sarangi 11/04/2025 08:36:00

Page 1: [2] Deleted Chandan Sarangi 11/04/2025 08:36:00

Page 1: [2] Deleted Chandan Sarangi 11/04/2025 08:36:00

Page 1: [2] Deleted Chandan Sarangi 11/04/2025 08:36:00

Page 1: [3] Deleted Chandan Sarangi 06/04/2025 07:15:00

Page 1: [3] Deleted Chandan Sarangi 06/04/2025 07:15:00

Page 1: [3] Deleted Chandan Sarangi 06/04/2025 07:15:00

Page 1: [3] Deleted Chandan Sarangi 06/04/2025 07:15:00

Page 1: [4] Deleted Chandan Sarangi 06/04/2025 07:13:00

Page 1: [4] Deleted Chandan Sarangi 06/04/2025 07:13:00

Page 1: [5] Deleted Chandan Sarangi 06/04/2025 07:15:00

Page 1: [5] Deleted Chandan Sarangi 06/04/2025 07:15:00

Page 1: [6] Deleted Chandan Sarangi 06/04/2025 07:17:00

Page 1: [7] Deleted Chandan Sarangi 06/04/2025 08:05:00

Page 1: [7] Deleted Chandan Sarangi 06/04/2025 08:05:00

Page 1: [8] Deleted Chandan Sarangi 06/04/2025 08:06:00

Page 1: [8] Deleted Chandan Sarangi 06/04/2025 08:06:00

Page 1: [9] Deleted Chandan Sarangi 11/04/2025 09:10:00

Page 1: [9] Deleted Chandan Sarangi 11/04/2025 09:10:00

Page 1: [9] Deleted	Chandan Sarangi	11/04/2025 09:10:00
---------------------	-----------------	---------------------

Page 1: [9] Deleted	Chandan Sarangi	11/04/2025 09:10:00
---------------------	-----------------	---------------------

Page 1: [10] Deleted	Dr. Saleem Ali	15/04/2025 20:33:00
----------------------	----------------	---------------------

Page 1: [10] Deleted	Dr. Saleem Ali	15/04/2025 20:33:00
----------------------	----------------	---------------------

Page 1: [10] Deleted	Dr. Saleem Ali	15/04/2025 20:33:00
----------------------	----------------	---------------------

Page 1: [10] Deleted	Dr. Saleem Ali	15/04/2025 20:33:00
----------------------	----------------	---------------------

Page 1: [11] Deleted	Chandan Sarangi	06/04/2025 08:25:00
----------------------	-----------------	---------------------

Page 1: [11] Deleted	Chandan Sarangi	06/04/2025 08:25:00
----------------------	-----------------	---------------------

Page 1: [11] Deleted	Chandan Sarangi	06/04/2025 08:25:00
----------------------	-----------------	---------------------

Page 1: [11] Deleted	Chandan Sarangi	06/04/2025 08:25:00
----------------------	-----------------	---------------------

Page 5: [12] Formatted	Dr. Saleem Ali	15/04/2025 20:33:00
------------------------	----------------	---------------------

Indent: First line: 1.27 cm

Page 5: [13] Formatted	Dr. Saleem Ali	15/04/2025 20:33:00
------------------------	----------------	---------------------

Font: Times New Roman, 10 pt, Ligatures: None

Page 5: [14] Formatted Dr. Saleem Ali 15/04/2025 20:33:00

Indent: First line: 1.27 cm

Page 5: [15] Deleted Chandan Sarangi 06/04/2025 11:19:00

Page 5: [16] Deleted Chandan Sarangi 06/04/2025 11:20:00

Page 5: [17] Deleted Chandan Sarangi 06/04/2025 11:28:00

Page 5: [18] Deleted Chandan Sarangi 06/04/2025 11:30:00

Page 5: [19] Deleted Chandan Sarangi 07/04/2025 07:12:00

Page 5: [20] Deleted Chandan Sarangi 06/04/2025 11:32:00

Page 5: [21] Deleted Dr. Saleem Ali 15/04/2025 20:45:00

Page 6: [22] Formatted Dr. Saleem Ali 07/04/2025 19:00:00

Font: Bold, Italic

Page 6: [22] Formatted Dr. Saleem Ali 07/04/2025 19:00:00

Font: Bold, Italic

Page 6: [22] Formatted Dr. Saleem Ali 07/04/2025 19:00:00

Font: Bold, Italic

Page 6: [22] Formatted Dr. Saleem Ali 07/04/2025 19:00:00

Font: Bold, Italic

Page 6: [23] Deleted Chandan Sarangi 06/04/2025 17:09:00

Page 6: [23] Deleted Chandan Sarangi 06/04/2025 17:09:00

Page 6: [24] Deleted Chandan Sarangi 06/04/2025 21:41:00

Page 6: [24] Deleted Chandan Sarangi 06/04/2025 21:41:00

Page 6: [24] Deleted Chandan Sarangi 06/04/2025 21:41:00

Page 6: [25] Deleted Dr. Saleem Ali 15/04/2025 20:33:00

Page 6: [25] Deleted Dr. Saleem Ali 15/04/2025 20:33:00

Page 6: [25] Deleted Dr. Saleem Ali 15/04/2025 20:33:00

Page 6: [26] Deleted Dr. Saleem Ali 15/04/2025 20:33:00

Page 6: [26] Deleted Dr. Saleem Ali 15/04/2025 20:33:00

Page 6: [26] Deleted Dr. Saleem Ali 15/04/2025 20:33:00

Page 6: [26] Deleted Dr. Saleem Ali 15/04/2025 20:33:00

Page 6: [27] Deleted Chandan Sarangi 06/04/2025 21:44:00

Page 6: [27] Deleted Chandan Sarangi 06/04/2025 21:44:00

Page 6: [28] Deleted Chandan Sarangi 06/04/2025 21:44:00

Page 6: [28] Deleted Chandan Sarangi 06/04/2025 21:44:00

Page 6: [29] Deleted Dr. Saleem Ali 07/04/2025 17:39:00

Page 6: [29] Deleted Dr. Saleem Ali 07/04/2025 17:39:00

Page 6: [30] Deleted Dr. Saleem Ali 07/04/2025 17:40:00

Page 6: [31] Formatted Dr. Saleem Ali 15/04/2025 20:33:00

Font:

Page 6: [31] Formatted Dr. Saleem Ali 15/04/2025 20:33:00

Font:

Page 6: [32] Deleted Dr. Saleem Ali 07/04/2025 17:41:00

Page 6: [32] Deleted Dr. Saleem Ali 07/04/2025 17:41:00

Page 6: [33] Formatted Dr. Saleem Ali 15/04/2025 20:33:00

Font color: Auto

Page 6: [33] Formatted Dr. Saleem Ali 15/04/2025 20:33:00

Font color: Auto

Page 6: [34] Deleted Chandan Sarangi 11/04/2025 09:42:00

Page 6: [34] Deleted Chandan Sarangi 11/04/2025 09:42:00

Page 6: [34] Deleted Chandan Sarangi 11/04/2025 09:42:00

Page 7: [35] Deleted Chandan Sarangi 07/04/2025 08:02:00

Page 7: [36] Deleted Chandan Sarangi 07/04/2025 08:45:00

Page 7: [37] Deleted Chandan Sarangi 07/04/2025 08:58:00

Page 7: [38] Deleted Dr. Saleem Ali 31/03/2025 19:47:00

Page 7: [39] Deleted Dr. Saleem Ali 10/04/2025 13:34:00

Page 7: [40] Deleted Dr. Saleem Ali 07/04/2025 17:42:00

Page 7: [41] Deleted Chandan Sarangi 07/04/2025 08:57:00

Page 7: [42] Deleted Chandan Sarangi 07/04/2025 08:58:00

Page 7: [43] Deleted Dr. Saleem Ali 15/04/2025 20:50:00

Page 7: [44] Deleted Chandan Sarangi 07/04/2025 08:16:00

Page 7: [45] Deleted Chandan Sarangi 11/04/2025 09:46:00

Page 7: [46] Deleted Chandan Sarangi 07/04/2025 12:52:00

Page 7: [47] Deleted Chandan Sarangi 11/04/2025 09:51:00

Page 8: [48] Deleted Chandan Sarangi 11/04/2025 10:58:00

Page 8: [49] Deleted Dr. Saleem Ali 07/04/2025 21:22:00

Page 8: [50] Formatted	Dr. Saleem Ali	15/04/2025 11:12:00
------------------------	----------------	---------------------

Not Highlight

Page 8: [50] Formatted	Dr. Saleem Ali	15/04/2025 11:12:00
------------------------	----------------	---------------------

Not Highlight

Page 8: [50] Formatted	Dr. Saleem Ali	15/04/2025 11:12:00
------------------------	----------------	---------------------

Not Highlight

Page 8: [50] Formatted	Dr. Saleem Ali	15/04/2025 11:12:00
------------------------	----------------	---------------------

Not Highlight

Page 8: [50] Formatted	Dr. Saleem Ali	15/04/2025 11:12:00
------------------------	----------------	---------------------

Not Highlight

Page 8: [50] Formatted	Dr. Saleem Ali	15/04/2025 11:12:00
------------------------	----------------	---------------------

Not Highlight

Page 8: [51] Formatted	Dr. Saleem Ali	15/04/2025 20:33:00
------------------------	----------------	---------------------

Font:

Page 8: [51] Formatted	Dr. Saleem Ali	15/04/2025 20:33:00
------------------------	----------------	---------------------

Font:

Page 8: [52] Formatted	Dr. Saleem Ali	15/04/2025 20:33:00
------------------------	----------------	---------------------

Font:

Page 8: [53] Deleted	Chandan Sarangi	11/04/2025 13:06:00
----------------------	-----------------	---------------------

Page 8: [53] Deleted	Chandan Sarangi	11/04/2025 13:06:00
----------------------	-----------------	---------------------

Page 8: [53] Deleted	Chandan Sarangi	11/04/2025 13:06:00
----------------------	-----------------	---------------------

Page 8: [54] Formatted	Dr. Saleem Ali	07/04/2025 19:00:00
------------------------	----------------	---------------------

Font: 10 pt, Not Bold

Page 8: [55] Deleted	Chandan Sarangi	11/04/2025 13:07:00
----------------------	-----------------	---------------------

Page 8: [55] Deleted	Chandan Sarangi	11/04/2025 13:07:00
----------------------	-----------------	---------------------

Page 8: [56] Deleted Dr. Saleem Ali 15/04/2025 11:27:00

Page 8: [56] Deleted Dr. Saleem Ali 15/04/2025 11:27:00

Page 8: [57] Deleted Chandan Sarangi 11/04/2025 14:37:00

Page 8: [58] Formatted Dr. Saleem Ali 07/04/2025 19:00:00

Font: 10 pt, Not Bold

Page 8: [59] Deleted Dr. Saleem Ali 15/04/2025 20:52:00

Page 8: [60] Deleted Dr. Saleem Ali 15/04/2025 20:33:00

Page 8: [61] Deleted Dr. Saleem Ali 31/03/2025 23:23:00

Page 8: [61] Deleted Dr. Saleem Ali 31/03/2025 23:23:00

Page 8: [61] Deleted Dr. Saleem Ali 31/03/2025 23:23:00

Page 8: [61] Deleted Dr. Saleem Ali 31/03/2025 23:23:00

Page 8: [61] Deleted Dr. Saleem Ali 31/03/2025 23:23:00

Page 8: [61] Deleted Dr. Saleem Ali 31/03/2025 23:23:00

Page 8: [61] Deleted Dr. Saleem Ali 31/03/2025 23:23:00

Page 8: [61] Deleted Dr. Saleem Ali 31/03/2025 23:23:00

Page 8: [61] Deleted Dr. Saleem Ali 31/03/2025 23:23:00

Page 8: [62] Formatted Dr. Saleem Ali 15/04/2025 20:33:00

Font:

Page 8: [63] Formatted Dr. Saleem Ali 15/04/2025 20:33:00

Indent: First line: 1.27 cm

Page 8: [64] Deleted Chandan Sarangi 12/04/2025 17:37:00

Page 8: [64] Deleted Chandan Sarangi 12/04/2025 17:37:00

Page 8: [65] Formatted Dr. Saleem Ali 15/04/2025 20:33:00

Font:

Page 8: [66] Formatted Dr. Saleem Ali 15/04/2025 20:33:00

Font:

Page 8: [67] Formatted Dr. Saleem Ali 15/04/2025 20:33:00

Font:

Page 8: [68] Formatted Dr. Saleem Ali 07/04/2025 19:00:00

Font: 10 pt, Not Bold

Page 8: [68] Formatted Dr. Saleem Ali 07/04/2025 19:00:00

Font: 10 pt, Not Bold

Page 8: [69] Formatted Dr. Saleem Ali 07/04/2025 19:00:00

Font: 10 pt, Not Bold

Page 8: [69] Formatted Dr. Saleem Ali 07/04/2025 19:00:00

Font: 10 pt, Not Bold

Page 8: [70] Formatted Dr. Saleem Ali 07/04/2025 19:00:00

Font: 10 pt, Not Bold

Page 8: [70] Formatted Dr. Saleem Ali 07/04/2025 19:00:00

Font: 10 pt, Not Bold

Page 8: [71] Formatted	Dr. Saleem Ali	07/04/2025 19:00:00
------------------------	----------------	---------------------

Font: 10 pt, Not Bold

Page 8: [71] Formatted	Dr. Saleem Ali	07/04/2025 19:00:00
------------------------	----------------	---------------------

Font: 10 pt, Not Bold

Page 8: [71] Formatted	Dr. Saleem Ali	07/04/2025 19:00:00
------------------------	----------------	---------------------

Font: 10 pt, Not Bold

Page 8: [72] Formatted	Dr. Saleem Ali	15/04/2025 20:33:00
------------------------	----------------	---------------------

Font:

Page 8: [73] Formatted	Dr. Saleem Ali	07/04/2025 19:00:00
------------------------	----------------	---------------------

Font: 10 pt, Not Bold

Page 8: [74] Formatted	Dr. Saleem Ali	15/04/2025 20:33:00
------------------------	----------------	---------------------

Font:

Page 8: [75] Deleted	Chandan Sarangi	11/04/2025 14:55:00
----------------------	-----------------	---------------------

Page 8: [76] Formatted	Dr. Saleem Ali	07/04/2025 19:00:00
------------------------	----------------	---------------------

Font: 10 pt, Not Bold

Page 8: [76] Formatted	Dr. Saleem Ali	07/04/2025 19:00:00
------------------------	----------------	---------------------

Font: 10 pt, Not Bold

Page 8: [77] Formatted	Dr. Saleem Ali	15/04/2025 20:33:00
------------------------	----------------	---------------------

Font:

Page 8: [77] Formatted	Dr. Saleem Ali	15/04/2025 20:33:00
------------------------	----------------	---------------------

Font:

Page 9: [78] Deleted	Chandan Sarangi	12/04/2025 17:47:00
----------------------	-----------------	---------------------

Page 9: [78] Deleted	Chandan Sarangi	12/04/2025 17:47:00
----------------------	-----------------	---------------------

Page 9: [78] Deleted	Chandan Sarangi	12/04/2025 17:47:00
----------------------	-----------------	---------------------

Page 9: [79] Formatted	Dr. Saleem Ali	15/04/2025 20:33:00
------------------------	----------------	---------------------

Font:

Page 9: [79] Formatted	Dr. Saleem Ali	15/04/2025 20:33:00
------------------------	----------------	---------------------

Font:

Page 9: [79] Formatted	Dr. Saleem Ali	15/04/2025 20:33:00
------------------------	----------------	---------------------

Font:

Page 9: [79] Formatted	Dr. Saleem Ali	15/04/2025 20:33:00
------------------------	----------------	---------------------

Font:

Page 9: [80] Deleted	Chandan Sarangi	12/04/2025 18:09:00
----------------------	-----------------	---------------------

Page 9: [80] Deleted	Chandan Sarangi	12/04/2025 18:09:00
----------------------	-----------------	---------------------

Page 9: [81] Deleted	Dr. Saleem Ali	31/03/2025 23:32:00
----------------------	----------------	---------------------

Page 9: [82] Deleted	Chandan Sarangi	12/04/2025 18:07:00
----------------------	-----------------	---------------------

Page 9: [83] Deleted	Chandan Sarangi	12/04/2025 18:10:00
----------------------	-----------------	---------------------

Page 9: [83] Deleted	Chandan Sarangi	12/04/2025 18:10:00
----------------------	-----------------	---------------------

Page 9: [83] Deleted	Chandan Sarangi	12/04/2025 18:10:00
----------------------	-----------------	---------------------

Page 9: [84] Formatted	Dr. Saleem Ali	07/04/2025 19:00:00
------------------------	----------------	---------------------

Font: 10 pt, Not Bold

Page 9: [84] Formatted	Dr. Saleem Ali	07/04/2025 19:00:00
------------------------	----------------	---------------------

Font: 10 pt, Not Bold

Page 9: [85] Deleted	Chandan Sarangi	12/04/2025 18:11:00
----------------------	-----------------	---------------------

Page 9: [85] Deleted	Chandan Sarangi	12/04/2025 18:11:00
----------------------	-----------------	---------------------

Page 9: [85] Deleted	Chandan Sarangi	12/04/2025 18:11:00
----------------------	-----------------	---------------------

Page 9: [85] Deleted Chandan Sarangi 12/04/2025 18:11:00

Page 9: [86] Deleted Chandan Sarangi 12/04/2025 18:12:00

Page 9: [86] Deleted Chandan Sarangi 12/04/2025 18:12:00

Page 9: [87] Deleted Chandan Sarangi 12/04/2025 22:29:00

Page 9: [87] Deleted Chandan Sarangi 12/04/2025 22:29:00

Page 9: [87] Deleted Chandan Sarangi 12/04/2025 22:29:00

Page 9: [87] Deleted Chandan Sarangi 12/04/2025 22:29:00

Page 9: [87] Deleted Chandan Sarangi 12/04/2025 22:29:00

Page 9: [87] Deleted Chandan Sarangi 12/04/2025 22:29:00

Page 9: [87] Deleted Chandan Sarangi 12/04/2025 22:29:00

Page 9: [87] Deleted Chandan Sarangi 12/04/2025 22:29:00

Page 9: [87] Deleted Chandan Sarangi 12/04/2025 22:29:00

Page 9: [87] Deleted Chandan Sarangi 12/04/2025 22:29:00

Page 9: [87] Deleted Chandan Sarangi 12/04/2025 22:29:00

Page 9: [87] Deleted Chandan Sarangi 12/04/2025 22:29:00

Page 9: [87] Deleted Chandan Sarangi 12/04/2025 22:29:00

Page 9: [87] Deleted Chandan Sarangi 12/04/2025 22:29:00

Page 9: [88] Deleted Dr. Saleem Ali 15/04/2025 20:57:00

Page 9: [89] Deleted Dr. Saleem Ali 15/04/2025 12:18:00

Page 9: [89] Deleted Dr. Saleem Ali 15/04/2025 12:18:00

Page 9: [90] Formatted Dr. Saleem Ali 15/04/2025 20:33:00

English (United Kingdom)

Page 9: [90] Formatted Dr. Saleem Ali 15/04/2025 20:33:00

English (United Kingdom)

Page 9: [90] Formatted Dr. Saleem Ali 15/04/2025 20:33:00

English (United Kingdom)

Page 9: [90] Formatted Dr. Saleem Ali 15/04/2025 20:33:00

English (United Kingdom)

Page 10: [91] Deleted Chandan Sarangi 12/04/2025 23:08:00

Page 10: [92] Deleted Chandan Sarangi 12/04/2025 23:08:00

Page 10: [93] Deleted Dr. Saleem Ali 01/04/2025 00:07:00

Page 10: [94] Deleted Chandan Sarangi 12/04/2025 23:12:00

Page 10: [95] Deleted	Dr. Saleem Ali	07/04/2025 18:22:00
-----------------------	----------------	---------------------

Page 10: [96] Deleted	Chandan Sarangi	12/04/2025 23:20:00
-----------------------	-----------------	---------------------

Page 11: [97] Formatted	Dr. Saleem Ali	15/04/2025 13:00:00
-------------------------	----------------	---------------------

Subscript

Page 11: [98] Deleted	Chandan Sarangi	13/04/2025 16:52:00
-----------------------	-----------------	---------------------

Page 11: [99] Deleted	Chandan Sarangi	13/04/2025 16:49:00
-----------------------	-----------------	---------------------

Page 11: [100] Deleted	Dr. Saleem Ali	15/04/2025 13:47:00
------------------------	----------------	---------------------

Page 11: [101] Formatted	Dr. Saleem Ali	15/04/2025 13:49:00
--------------------------	----------------	---------------------

Subscript

Page 11: [102] Deleted	Chandan Sarangi	12/04/2025 23:22:00
------------------------	-----------------	---------------------

Page 11: [103] Deleted	Chandan Sarangi	13/04/2025 17:29:00
------------------------	-----------------	---------------------

Page 11: [104] Formatted	Dr. Saleem Ali	15/04/2025 17:16:00
--------------------------	----------------	---------------------

Subscript

Page 11: [105] Formatted	Dr. Saleem Ali	15/04/2025 17:20:00
--------------------------	----------------	---------------------

Subscript

Page 12: [106] Deleted	Dr. Saleem Ali	15/04/2025 17:24:00
------------------------	----------------	---------------------

Page 14: [107] Deleted	Dr. Saleem Ali	14/04/2025 23:57:00
------------------------	----------------	---------------------

Page 14: [108] Deleted	Dr. Saleem Ali	14/04/2025 23:09:00
------------------------	----------------	---------------------